Final Technical Report Submission

1. USGS Award Number

G09AP00135

2. Title of award

Vector-valued Probabilistic Seismic Hazard Analysis of Correlated Ground Motion Parameters

3. Authors

- Paolo Bazzurro
  388 Market St. suite 750 San Francisco, CA 94111
  Office Telephone: 415-912-3111
  Office Fax: 415-912-3112
  Email: pbazzurro@air-worldwide.com
- Jaesung Park
  388 Market St. suite 750 San Francisco, CA 94111
  Office Telephone: 415-912-3111
  Office Fax: 415-912-3112
  Email: jpark@air-worldwide.com
- Polsak Tothong
  Email: ptothong@gmail.com

4. Terms

Start Date: 08/01/2009
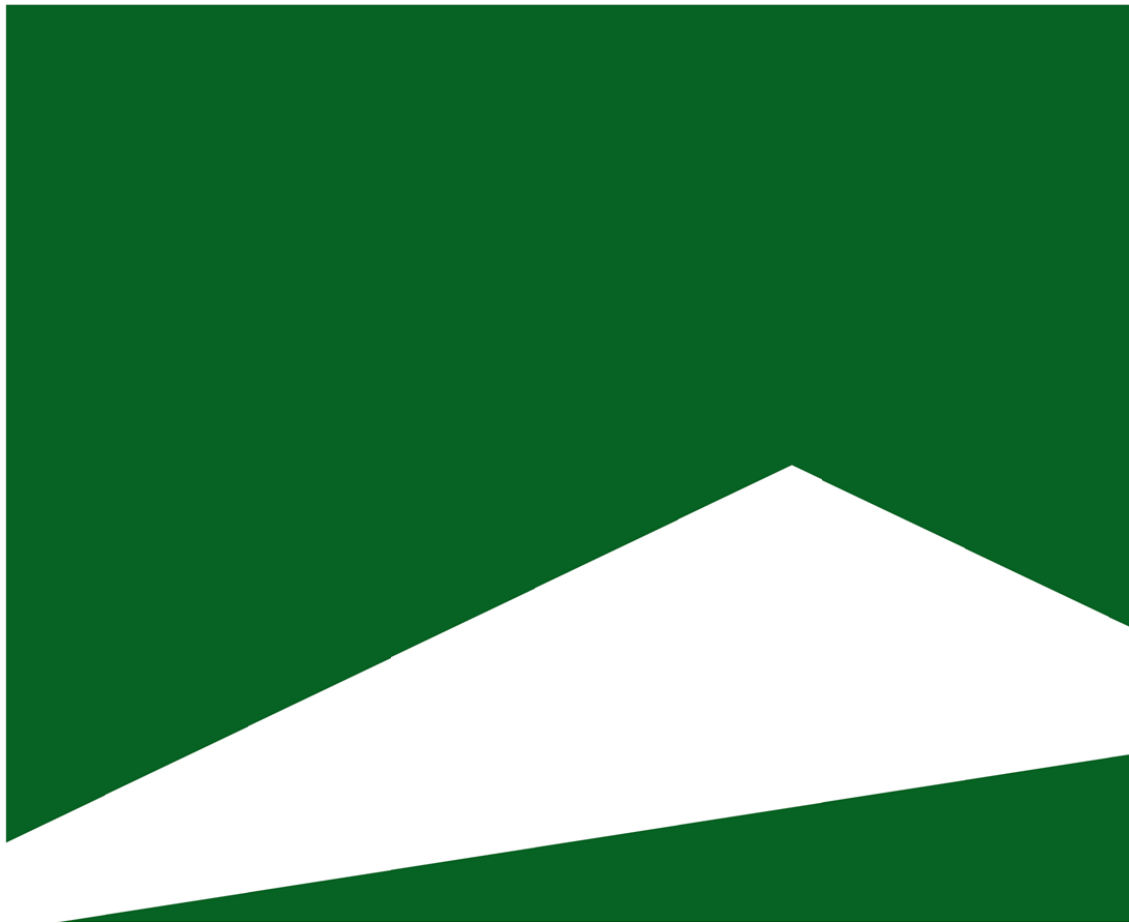End Date : 07/31/2010

Abstract

After many years of development in academia, performance-based earthquake engineering (PBEE) has become a common tool in industry for assessing the response of buildings and other structures subjected to seismic loading. Studies based on PBEE are used by a variety of stakeholders. Building owners, for example, use the results of these studies to decide whether to retrofit buildings and/or whether to invest in earthquake insurance. Lending institutions use them to decide whether to grant or deny a loan. Insurers use them to decide whether to underwrite earthquake insurance for a structure at a particular site and to determine an appropriate premium. Regardless of the application, it is critical that estimates of the likelihood that a structure's response exceeds a given level of severity, ranging from the onset of damage to incipient collapse, be as accurate as reasonably possible.

The three main aspects of PBEE are (1) evaluation of seismic hazard, (2) assessment of the response of the structure for any given level of ground shaking, and (3) computation of consequences potentially induced by any state of damage predicted by the response analysis. Such consequences are usually measured in terms of monetary losses, downtime and casualties. To increase the accuracy of the response prediction, engineers have recently taken advantage of the computational capabilities of modern computers by building more realistic two-dimensional and three-dimensional numerical models. The response of these complicated models is better gauged by monitoring multiple behavioural metrics, such as maximum interstory drifts in both the longitudinal and transverse directions, and the maximum story acceleration along the height of the structure. To predict the values of such response measures, multiple intensity measures (IMs) of the ground motion in both horizontal (and sometimes vertical) directions are necessary. Hence, many researchers have recognized the need for estimating the *joint* site hazard of the predicted ground motion parameters of interest, which is a complicated task since these parameters are generally correlated.

The seminal methodology to evaluate joint seismic hazard, which was co-authored by the PI of this proposal, was introduced in 1998 and was called Vector Probabilistic Seismic Hazard Analysis (VPSHA). This method, which is herein called the "direct method", is based on numerical integration of the joint Gaussian distribution of ground motion parameters generated at a site by an earthquake of given characteristics. Despite the long availability of the methodology, VPSHA has been rarely used in practice mainly because the three VPSHA computer programs in existence (Bazzurro, 1998; Thio, 2003; Gülerce and Abrahamson, 2010) have inadequate documentation, are limited to two parameters, and are unable to identify the scenarios that control the joint hazard via the so-called "disaggregation" procedure. These shortcomings have severely hindered their use. To circumvent these problems, engineers have used scalar PSHAs for single ground motion parameters that are combinations of multiple ones (e.g., the geometric mean of the spectral accelerations at the first period of vibration in the two main horizontal directions of a building).

To help promote the use of VPSHA, this study develops a methodology, herein called the "indirect approach", which allows the computation of the joint hazard using *any standard scalar* PSHA software. In addition, the method makes use of the covariance matrix of the ground motion parameters for which the joint hazard is sought, and the disaggregated *scalar* site hazard for all the ground motion parameters considered. The empirically-derived covariance matrix for many ground motion parameters is currently available in the literature (e.g., Inoue, 1990). This indirect approach to VPSHA is more computationally efficient as compared to the direct method. The indirect method can accommodate up to five or six random variables with current desktop computer limitations without significant loss of accuracy and can determine the disaggregation of the joint hazard. Note that the direct integration method, which is analyzed in this study for the purposes of validating the proposed indirect approach, can only handle up to three variables, and requires extremely costly computations. The computationally efficient indirect method could be easily coupled with the hazard and disaggregation results from USGS scalar hazard maps or OpenSHA to produce joint hazard estimates at any site.

Vector-Valued Probabilistic Seismic Hazard Analysis of Correlated Ground Motion Parameters

Technical Report Submitted to the U.S.G.S.

Authors:
Paolo Bazzurro
Jaesung Park
Polsak Tothong

October 21, 2010

Table of Contents

EXECUTIVE SUMMARY

After many years of development in academia, performance-based earthquake engineering (PBEE) has become a common tool in industry for assessing the response of buildings and other structures subjected to seismic loading. Studies based on PBEE are used by a variety of stakeholders. Building owners, for example, use the results of these studies to decide whether to retrofit buildings and/or whether to invest in earthquake insurance. Lending institutions use them to decide whether to grant or deny a loan. Insurers use them to decide whether to underwrite earthquake insurance for a structure at a particular site and to determine an appropriate premium. Regardless of the application, it is critical that estimates of the likelihood that a structure's response exceeds a given level of severity, ranging from the onset of damage to incipient collapse, be as accurate as reasonably possible.

The three main aspects of PBEE are (1) evaluation of seismic hazard, (2) assessment of the response of the structure for any given level of ground shaking, and (3) computation of consequences potentially induced by any state of damage predicted by the response analysis. Such consequences are usually measured in terms of monetary losses, downtime and casualties. To increase the accuracy of the response prediction, engineers have recently taken advantage of the computational capabilities of modern computers by building more realistic two-dimensional and three-dimensional numerical models. The response of these complicated models is better gauged by monitoring multiple behavioural metrics, such as maximum interstory drifts in both the longitudinal and transverse directions, and the maximum story acceleration along the height of the structure. To predict the values of such response measures, multiple intensity measures (IMs) of the ground motion in both horizontal (and sometimes vertical) directions are necessary. Hence, many researchers have recognized the need for estimating the *joint* site hazard of the predicted ground motion parameters of interest, which is a complicated task since these parameters are generally correlated.

The seminal methodology to evaluate joint seismic hazard, which was co-authored by the PI of this proposal, was introduced in 1998 and was called Vector Probabilistic Seismic Hazard Analysis (VPSHA). This method, which is herein called the "direct method", is based on numerical integration of the joint Gaussian distribution of ground motion parameters generated at a site by an earthquake of given characteristics. Despite the long availability of the methodology, VPSHA has been rarely used in practice mainly because the three VPSHA computer programs in existence (Bazzurro, 1998; Thio, 2003; Gülerce and Abrahamson, 2010) have inadequate documentation, are limited to two parameters, and are unable to identify the scenarios that control the joint hazard via the so-called "disaggregation" procedure. These shortcomings have severely hindered their use. To circumvent these problems, engineers have used scalar PSHAs for single ground motion parameters that are combinations of multiple ones (e.g., the geometric mean of the spectral accelerations at the first period of vibration in the two main horizontal directions of a building).

To help promoting the use of VPSHA, this study develops a methodology, herein called the "indirect approach", which allows the computation of the joint hazard using *any standard scalar* PSHA software. In addition, the method makes use of the covariance matrix of the ground motion parameters for which the joint hazard is sought, and the disaggregated *scalar* site hazard for all the ground motion parameters considered. The empirically-derived covariance matrix for many ground motion parameters is currently available in the literature. This indirect approach to VPSHA is more computationally efficient as compared to the direct method based on the integration of multivariate Gaussian distributions. The indirect method can accommodate up to five or six random variables with current desktop computer limitations without significant loss of accuracy and can disaggregate the joint hazard. Note that the direct integration method, which is analyzed in this study only for the purposes of validating the proposed indirect approach, can only handle up to three variables, and requires extremely costly computations. The computationally efficient indirect method could be easily coupled with the hazard and disaggregation results from USGS scalar hazard maps or OpenSHA to produce joint hazard estimates at any site.

1. Motivation

After many years of incubation in academia, performance-based earthquake engineering (PBEE) for assessing the response of buildings and other structures subjected to seismic loading has become commonplace in industry. Studies based on PBEE are used by a variety of stakeholders. Building owners, for example, use the results of these studies to decide whether to retrofit buildings and/or invest in earthquake insurance. Lending institutions use them to decide whether to grant or deny a loan. Insurers use them to decide whether to underwrite earthquake insurance for a structure at a particular site and to determine an appropriate premium. Structural engineers use it to design structural components to withstand forces and control displacements induced by target design ground motions with a margin of safety corresponding to well-performing, code-compliant structures. A recent and important example where PBEE has been instrumental is in the design of buildings taller than the maximum height of 240ft allowed by building codes in the main cities along the U.S. West Coast (e.g., Maffei and Yuen, 2007). Regardless of the application, it is critical that estimates of the likelihood that a structure's response exceeds a given level of severity, ranging from onset of damage to incipient collapse, be as accurate as reasonably possible.

The three main aspects of PBEE (e.g., Deierlein *et al.*, 2003) are –

a) evaluation of the seismic hazard;
b) assessment of the response of the structure for any given level of ground shaking; and
c) computation of the monetary losses of the structure in any state of damage predicted by the estimated response.

To increase the accuracy of estimating the structure's response, engineers have recently started to take advantage of the computational capabilities of modern computers by developing more realistic two-dimensional (2D) and three-dimensional (3D) numerical models (e.g., see Figure 1). These computer models are subjected to many different ground motions of different intensities to assess the structure's performance. Statistical tools are typically used to provide functional relationships between the intensity measures of the ground shaking and measures of response that are associated with required levels of performance (e.g., life safety or collapse).
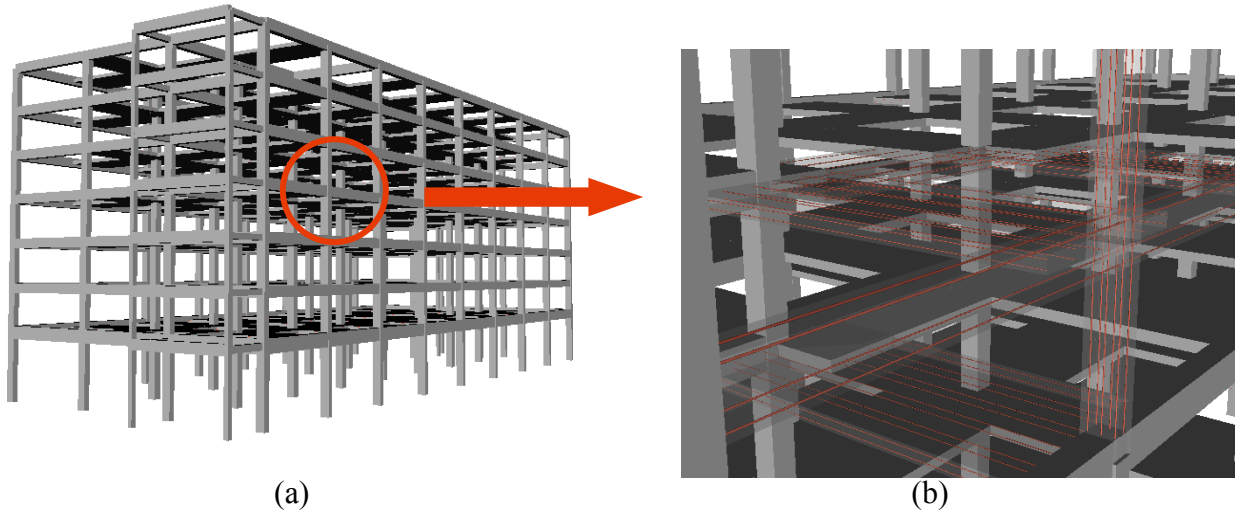

(a)   (b)

Figure 1 A three-dimensional model (developed by the authors) of a 7-story reinforced concrete frame (a) with details of the steel reinforcement in the slabs and columns (b).

The complex response of these realistic models, however, is better estimated by monitoring multiple response measures, such as the interstory drift both in longitudinal direction, δ_L, and in transverse direction, δ_T, as well as the absolute acceleration at each story. The maximum values of these measures

are good indicators of the physical damage (e.g., yielding and/or collapse) expected in the structure, as well as estimated damage to its contents. Estimates of the maximum values of these response measures are better predicted by a pool of IMs from ground motions in both horizontal (and sometimes vertical) directions, rather than by a single measure, as was done in the past (e.g., horizontal peak ground acceleration, PGA). For example, a good predictor of δ_L may be the spectral acceleration at the first period of vibration in the structure's longitudinal direction $S_a(T_L)$ and, similarly, δ_T may be well predicted by $S_a(T_T)$, the spectral acceleration in the structure's transverse direction. The collapse of a building, however, is more likely to happen when *both δ_L and δ_T*, and therefore $S_a(T_L)$ *and $S_a(T_T)$*, are large, rather than when either one is large.

It can be argued that quantification of the *joint* hazard of both $S_a(T_L)$ and $S_a(T_T)$ is very useful if not critical. Conventional scalar PSHA, however, computes the mean rate of occurrence (or exceedance) of $S_a(T_L)$ and $S_a(T_T)$ and other IMs separately, not jointly. An engineer must somehow combine this information to accurately evaluate the likelihood that a building will experience different levels of response and eventually whether it will collapse or not. The building response in the two horizontal directions, and the IMs $S_a(T_L)$ and $S_a(T_T)$, as well as others, are in general correlated, which makes the computation of the joint site hazard more complex. The desired improvement in the accuracy of structure's response, therefore, comes at a price.

The seminal methodology to evaluate joint seismic hazard was introduced in 1998 (Bazzurro, 1998; Bazzurro and Cornell, 2001 and 2002) and was called Vector-valued Probabilistic Seismic Hazard Analysis (VPSHA). Despite the long-term availability of the methodology, VPSHA has been rarely used in practice mainly because the three VPSHA computer programs currently in existence (Bazzurro, 1998; Thio, 2003; Gülerce and Abrahamson, 2010) have inadequate documentation, are limited to two IMs, and are unable to identify the scenarios that control the joint hazard via the so-called "disaggregation" procedure. Disaggregation is used in practical applications, among other things, to identify the earthquake scenarios that drive the hazard and to select appropriate ground motion records for structural response estimation that are consistent with such scenarios. These shortcomings have severely limited the use of VPSHA. To partially circumvent the problem, engineers have used scalar PSHA for single ground motion IMs that are combination of multiple ones (e.g., the geometric mean of the spectral accelerations at the first period of vibration in the two main horizontal directions of the building) - (Luco *et al*., 2005a; Luco and Cornell, 2007). However, this procedure is less effective than considering single ground motion IMs in the response prediction (step b in PBEE – see above) and accounting for the *joint* hazard of a pool of IMs when computing the risk (step c in PBEE).

To help promoting the use of VPSHA, a methodology has been developed and implemented that allows the computation of the joint hazard using results from *any standard scalar* PSHA software. This indirect approach to VPSHA is more computationally efficient than the original VPSHA direct integration method. In addition, the indirect method has other important advantages over the direct integration method, as it can (a) accommodate up to five or six random variables (RVs) under current desktop computer limitations without significant loss of accuracy and (b) disaggregate the joint hazard. The direct integration method, which was expanded to accommodate more than two RVs in this study, can only handle up to three variables without extremely expensive computations. For example, the run time for the direct method, used in one of the analysis presented in this study, ranged from approximately 800 hours for the 3D case to more than 30,000 hours for 4D case[1] with a modern desktop computer with at least 2GHz of processor speed.

Section 2 of this report explains how the original VPSHA framework was expanded beyond the computation of the joint hazard for two ground motion IMs while Section 3 presents the details of the proposed indirect approach to VPSHA. Section 4 outlines the results of the VPSHA for two sites, one in

---

[1] After we realized the amount of computations needed to complete the analysis, we terminated it and did not collect the results.

the San Francisco Bay Area and one in the Los Angeles area. Section 5 presents the results of a sensitivity analysis on the number and size of bins selected to discretize the domain of the RVs involved (namely, magnitude M, source-to-site distance R, and the ground motion IMs). Section 6 shows the disaggregation of M and R in the joint hazard. Finally, Section 7 summarizes the main results of this study and provides suggestions for future work.

The relevance of this study for reducing losses from earthquakes is direct, as it is a more comprehensive evaluation of the seismic hazard at a structure's site. Until now, most seismic risk analyses were conducted by coupling hazard and response analyses via a single ground motion IM, selected as a pinch point between the hazard and the structure's response estimation. Such a link has traditionally used PGA or spectral acceleration at a given period in one of the two horizontal directions of the ground motion. Many researchers have shown (Bazzurro, 1998; Luco and Cornell, 2000; Bazzurro and Cornell, 2002; Bazzurro and Luco, 2004 and 2005; Luco *et al.*, 2005a and 2005b, among others) that using more than one ground motion IM substantially improves the accuracy of the response prediction, especially for mid-rise and high-rise buildings. Multiple ground motion IMs can, in theory, be included in the hazard using the VPSHA approach, but its practical implementation has obstacles that this study attempts to mitigate. The systematic use of VPSHA will undoubtedly increase the accuracy of seismic risk analyses of existing structures and refine the design of new ones. Improved structural risk assessment of single structure is the first step in mitigating seismic risk for the inventory of buildings at large.

2. Direct Approach to VPSHA based on Numerical Integration

The original methodology for computing the joint hazard of multiple dependent RVs (Bazzurro, 1998; Bazzurro and Cornell, 2001 and 2002) is based on direct integration of the joint probability density function (pdf) of the ground motion IMs (e.g., PGA and $S_a(1.0s)$) generated by each earthquake considered in the analysis. The joint hazard of correlated IMs at a site is computed separately for each earthquake scenario, and the total hazard is obtained by summing the contributions from all scenarios weighted by their occurrence rates. This method contains no approximation besides the implicit numerical accuracy of the integration solver. This so-called "direct method" is considered in this report (1) to obtain a set of joint hazard results for as many ground motion IMs as possible to be used as a benchmark to validate the results from the indirect method and gauge their accuracy, and (2) to ascertain how many RVs this method could accommodate with modern computation capabilities.

The joint pdf, conditional on the parameters of the earthquake (i.e., M, R, the rupture mechanism, and the soil conditions), can be computed with the knowledge of ground motion prediction equations (GMPEs) for IMs involved and with their variance-covariance matrix. Inoue (1990) and, more recently, Baker and Cornell (2006), Baker and Jayaram (2008) and Goda and Hong (2008), have empirically derived the correlation structure for spectral accelerations with different periods (Figure 2a) and different accelerogram orientations. Jayaram and Baker (2008) showed that the joint probability density function of correlated IMs generated by the same earthquake follows a multinomial lognormal distribution. For example, Figure 2b shows the contours of the joint pdf for $S_a(1.0s)$ and $S_a(0.3s)$ generated at a site with V_s^{30}=760 m/s located 7km from a M_w=7.3 event with a strike-slip mechanism as predicted by the GMPE by Boore and Atkinson (2008). According to Baker and Jayaram (2008), the correlation coefficient for $S_a(1.0s)$ and $S_a(0.3s)$ is 0.5735 for this particular case. Hence, direct integration is conceptually straightforward but numerically challenging, especially when (a) high precision in the tails of the distribution is sought; (b) the number of earthquake scenarios is large, which is usually the case in realistic applications; and (c) the number of IMs exceeds 3 or 4. In fact, before this study, the only three VPSHA codes in existence (Bazzurro, 1998; Thio, 2003; Gülerce and Abrahamson, 2010) were limited to only two RVs.
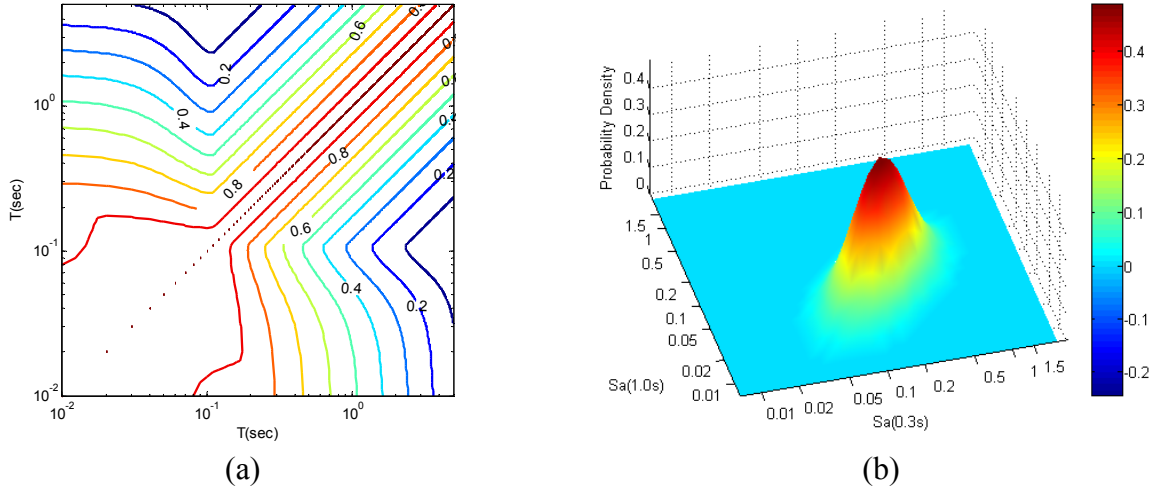
(a)   (b)

Figure 2 (a) The variance-covariance structure of spectral accelerations at different periods in a random horizontal component of a ground motion (Jayaram and Baker, 2008) and (b) the joint pdf for $S_a(1.0s)$ and $S_a(0.3s)$ for a scenario earthquake.

This study has developed a VPSHA software code in C++ that uses numerical integration techniques. The integration algorithm is based on a quasi-Monte Carlo integration algorithm developed by Genz and Bretz (1999 and 2002). Section 4 shows two realistic applications where this code was used.

3. Indirect Approach to VPSHA

Under the rational of joint lognormality mentioned above, the joint mean rate density (MRD - for definition and details, see Bazzurro and Cornell, 2002) or, similarly, the mean annual rate (MAR) of occurrence, of any combination of values of a pool of ground motion IMs, can be computed with the knowledge of the following inputs:

1. *Site-specific seismic hazard curves for all the ground motion IMs considered* - The vector of ground motion IMs is denoted herein as S, where the bold character indicates that the quantity is a vector. This vector could include, for example, three parameters: the spectral acceleration at two different periods in one of the horizontal directions, and at one period in the orthogonal horizontal direction. These periods could correspond to the first and second mode of vibrations of a building in the longitudinal directions and the first mode in the transverse direction. The three hazard curves corresponding to these periods can be obtained with any standard PSHA code.
2. *The variance-covariance matrix of all the ground motion IMs* - The empirically-derived variance matrix is available in the literature and was discussed in Section 2 (e.g., recall Figure 2a).
3. *The disaggregation results from scalar PSHA* - The joint distributions of all the basic variables, X, including M, R, the style of faulting, the distance to the top of the co-seismic rupture, and all other variables required by the GMPE of choice to compute the ground motion, conditional on the value of one or more ground motion parameters, is a straightforward extension of the disaggregation results routinely available from standard scalar PSHA codes (see Figure 3 for an example). As shown below, the necessary modifications are conceptually simple and involve only disaggregation of the site hazard in terms of some additional RVs beyond M and R as done in the past.
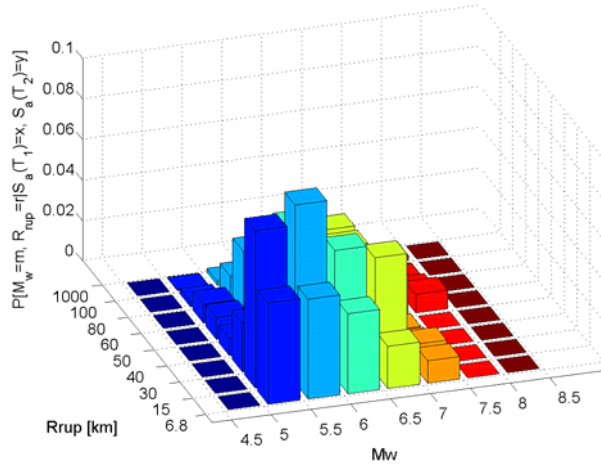
Figure 3 Contribution to the rate of equaling S_a(1s)=0.4g due to events of different M and R for a site in Southern California.

For brevity, details of the methodology are presented below for the case of only three IMs, which in this case are spectral accelerations. This approach, which requires some straightforward matrix algebra, is scalable to a larger number of RVs (see Eq. 4 to come) and can include any other ground motion parameters (e.g., duration, near-source forward-directivity pulse period) if the proper correlation structure and prediction equations are available. For simplicity, the RVs are treated as discrete rather than continuous quantities.

Let S=[S_{a1};S_{a2};S_{a3}] denote the vector of RVs for which we seek to obtain the joint hazard and MAR[S_{a1};S_{a2};S_{a3}] = MAR$_{Sa1;Sa2;Sa3}$(a_1;a_2;a_3) the mean annual rate of occurrence of the three spectral acceleration quantities S_{a1}, S_{a2}, and S_{a3} in the neighborhood of any combination of three values a_1, a_2, and a_3, respectively. Note that S_{a1};S_{a2};S_{a3} represents the natural logarithm of the spectral accelerations; the logarithm operator has been dropped herein to avoid lengthy notations. MAR[S_{a1};S_{a2};S_{a3}] could, for example, denote the MAR of observing at a building site values in the neighborhood of 1.0g, 1.5g, and 0.8g for the spectral acceleration quantities at the periods of the first and second modes of vibration in the building longitudinal direction and the spectral acceleration at the period of the first mode in the building transverse direction. These spectral acceleration values may be related to the onset of an important structural limit-state determined from a statistical analysis of the response of a structure subjected to many ground motion records. Then, using the theorem of total probability, one can express the following:

$$MAR[S_{a1}; S_{a2}; S_{a3}] = P[S_{a1}|S_{a2}; S_{a3}] \cdot P[S_{a2}|S_{a3}] \cdot MAR[S_{a3}]$$ (Eq. 1)

Where:

1. $P[S_{a1}|S_{a2}; S_{a3}] = \sum_X P[S_{a1}|S_{a2}; S_{a3}; X] \cdot P[X|S_{a2}; S_{a3}]$ (Eq. 2)

- Equation 2 represents the conditional distribution of S_{a1} given S_{a2} and S_{a3}. This term can be numerically computed by conditioning it to the pool of variables X in a standard PSHA that appear in the selected ground motion prediction equation and integrating over all possible values of X, as shown on the right hand side of Eq. 2. Exploiting the joint lognormality of S, for every possible value of X, the quantity $P[S_{a1}|S_{a2}; S_{a3}; X]$ can be computed simply with the knowledge of the variance-covariance matrix of S_{a1}, S_{a2}, and S_{a3}(e.g., from Baker and Cornell, 2006) and the ground motion prediction equation of choice. Further details of the mathematics are provided below. $P[X|S_{a2}; S_{a3}]$, which is the probability of X, conditional on the values of S_{a2} and S_{a3}, can be obtained via disaggregation and Bayes theorem as follows:

$$P[X|S_{a2};S_{a3}] = \frac{P[X,S_{a2}|S_{a3}]}{\sum_X P[S_{a2}|S_{a3};X] \cdot P[X|S_{a3}]} = \frac{P[S_{a2}|S_{a3};X] \cdot P[X|S_{a3}]}{P[S_{a2}|S_{a3}]}$$

Where:

- $P[X|S_{a3}]$ can be derived using conventional scalar PSHA disaggregation.
- $P[S_{a2}|S_{a3};X]$, similarly as for the $P[S_{a1}|S_{a2};S_{a3};X]$ term above, can be computed with simply the knowledge of the variance-covariance matrix of, S_{a2}, and S_{a3}, and the GMPE of choice.

2. $P[S_{a2}|S_{a3}] = \sum_X P[S_{a2}|S_{a3};X] \cdot P[X|S_{a3}]$ can be evaluated as explained above.
3. $MAR[S_{a3}]$ is the absolute value of the differential of the conventional seismic hazard curve for the scalar quantity S_{a3} at the site.

After some simplifications, Eq. 1 can be rewritten as follows:

$$MAR[S_{a1};S_{a2};S_{a3}] = MAR[S_{a3}] \cdot \sum_X P[S_{a1}|S_{a2};S_{a3};X] \cdot P[S_{a2}|S_{a3};X] \, P[X|S_{a3}] \qquad \text{(Eq. 3)}$$

The two first conditional terms in Eq. 3 (i.e., $P[S_{a1}|S_{a2};S_{a3};X]$ and $P[S_{a2}|S_{a3};X]$) can be easily evaluated using the multi-variate normal distribution theorem. In general, if $S = [S_{a1}, S_{a2}, \ldots, S_{an}]^T$ is denoted as the vector of the natural logarithm of the random variables for which the joint hazard is sought, then S is jointly normally distributed with mean μ and variance-covariance matrix $\sum$, i.e., in mathematical terms $S = \sim N(\mu, \sum)$. If S is partitioned into two vectors, $S_1 = [S_{a1}, S_{a2}, \ldots, S_{ak}]^T$ and $S_2 = [S_{ak+1}, S_{ak+2}, \ldots, S_{an}]^T$, where S_2 comprises the conditioning variables (in the example above $S_1 = [S_{a1}]^T$ and $S_2 = [S_{a2}, S_{a3}]^T$), one can write the following:

$$S = \begin{bmatrix} S_1 \\ S_2 \end{bmatrix} \sim N\left(\begin{bmatrix} \mu_1 \\ \mu_2 \end{bmatrix}, \begin{bmatrix} \sum_{11} & \sum_{12} \\ \sum_{21} & \sum_{22} \end{bmatrix} \right)$$

For jointly normal distribution, the conditional mean and variance can be determined as

$$S_1|S_2 = \sim N(\mu_{1|2}, \Sigma_{1|2})$$
$$\mu_{1|2} = \mu_1 + \Sigma_{12}\Sigma_{22}^{-1}(S_2 - \mu_2); \ \Sigma_{1|2} = \Sigma_{11} - \Sigma_{12}\Sigma_{22}^{-1}\Sigma_{21}$$

Eq. 3 can be generalized to *n* variables as follows:

$$MAR[S_{a1};S_{a2};S_{a3};\cdots;S_{an-1};S_{an}] =$$
$$\sum_X P[S_{a1}|S_{a2};S_{a3};\cdots;S_{an-1};S_{an};X] \cdot P[S_{a2}|S_{a3};\cdots;S_{an-1};S_{an};X] \cdot$$
$$P[Sa3|Sa4;\cdots;San-1;San;X]\cdots P[San-1|San;X] \cdot P[X|San] \cdot MAR[San] \qquad \text{(Eq. 4)}$$

This VPSHA methodology is used herein to evaluate the joint hazard of two sites of different hazard conditions (refer Section 4) for a vector containing up to five spectral acceleration values. The joint hazard will also be disaggregated on the vector parameters X.

4. Application of VPSHA

This section presents the application of the direct and indirect approaches of VPSHA to one site in the San Francisco Bay Area and another in the Los Angeles area. Unless noted otherwise, the results shown below were obtained using a very fine discretization of the domains of the RVs involved: (a) 160 earthquake magnitude bins ranging from 5.5 to 8.2, with a bin size of 0.02 magnitude units; (b) 101 source distance bins ranging from 0 to 200 km, with a bin size of 2.0 km; and (c) 93 intensity measure(s) bins ranging from -7 to 2.2 in natural log space (i.e., from 0.001g to about 9g), with a bin size of 0.2. This fine granularity was chosen to test the accuracy of the indirect method versus the "exact" results of the direct method. The IMs used are the linear elastic 5%-damped spectral accelerations $S_a(0.3s)$, $S_a(0.6s)$, $S_a(0.9s)$, $S_a(1.0s)$, and $S_a(2.0s)$.

4.1 Stanford University site

All the spectral quantities considered for this site were probabilistically computed using the GMPE of Abrahamson and Silva (1997) for shallow crustal events. Although this GMPE equation is obsolete, it is used in this analysis because it is simpler than the modern suite of equations developed for the Next Generation of Attenuation (NGA) project (Abrahamson *et al.*, 2008) and its use permits disaggregating the hazard with the indirect method for a smaller pool of variables, X=[M, R, rupture mechanism], where R here is the shortest distance between the source and the site. An additional simplification adopted in this case study is the assumption that all the earthquakes in the seismicity model (i.e. those of the San Francisco Bay Area) were generated by a strike-slip rupture mechanism. This additional assumption eliminates the need for rupture mechanism bookkeeping when disaggregating the site hazard in terms of M and R. These two simplifications will be relaxed in the subsequent case study for the Van Nuys site near Los Angeles, which is presented in the next subsection.

4.1.1 2D joint MAR of occurrence of $S_a(0.3s)$ and $S_a(1.0s)$

The joint mean annual rate (MAR) of occurrence for pairs of $S_a(0.3s)$ and $S_a(1.0s)$ values, obtained via the direct integration approach and the indirect approach, is shown in Figure 4. In the indirect approach, $S_a(1.0s)$ is the conditioning variable while $S_a(0.3s)$ is the conditioned variable in the 2D version of Eq. 4.

A visual comparison of Figure 4 shows that the MARs obtained via the indirect approach is virtually identical to the "exact" one computed by direct integration. The ratio of the MAR from these two analyses, plotted in Figure 5, shows that for all combinations of engineering significance, the error is within ±2%. The error reaches 10% only for the combinations of values whose occurrence rates are much less than 10^{-4} (i.e., very large $S_a(0.3s)$ values and small to moderate $S_a(1.0s)$ values).

The marginal complementary cumulative distributions of the joint MAR in Figure 4 are simply the customary 1D seismic hazard curves. From an inspection of Figure 6, it is evident that the marginal distributions, extracted from the joint MAR of both approaches, are consistent with those from a conventional scalar PSHA, as expected. The hazard curves from the direct approach and the hazard curve from the c*onditioning* variable in the indirect approach are (here $S_a(1.0s)$), of course, identical. The hazard curve for the *conditioned* variable from the indirect approach (here $S_a(0.3s)$), however, carries some discrepancies due to the width of the RV bins. In this case, the error ranges from about zero at $S_a(0.3s)$=1.0g to about 3% at $S_a(0.3s)$=5.0g (corresponding to an annual mean rate of exceedance lower than 10^{-5} for this site). Nevertheless, these errors are well below the threshold of concern.
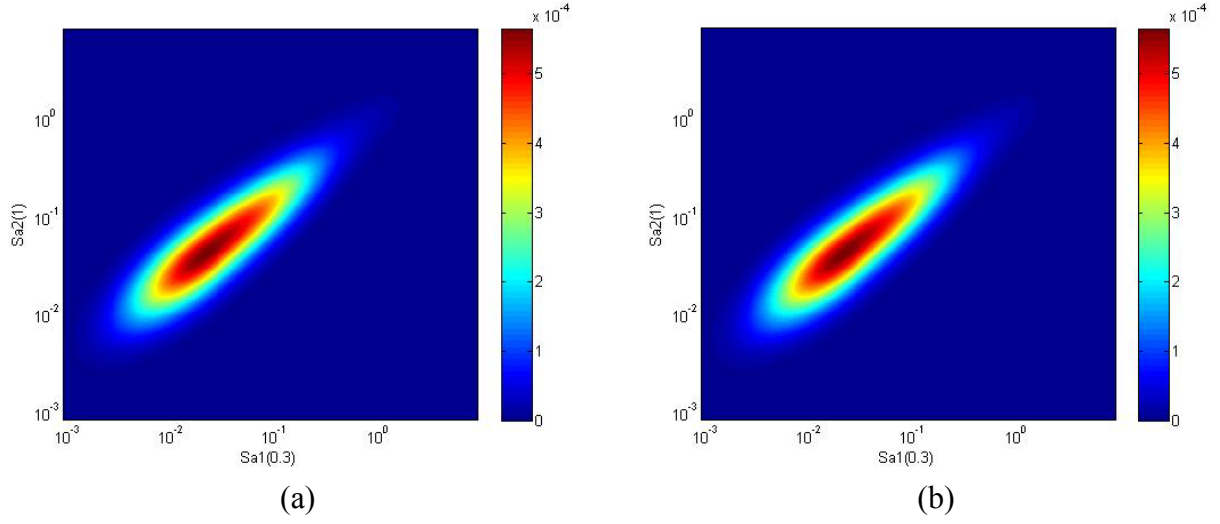
(a) (b)

Figure 4 Joint MAR of S_a(0.3s) and S_a(1.0s) obtained via (a) the direct integration method and (b) the indirect method.
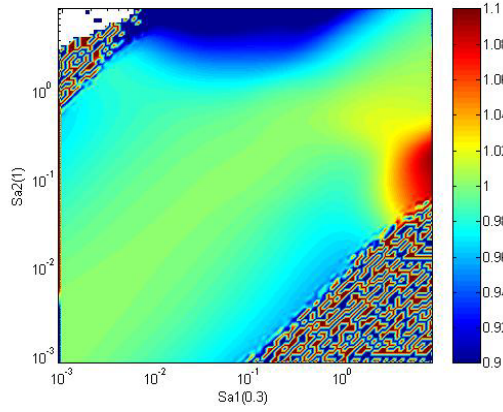

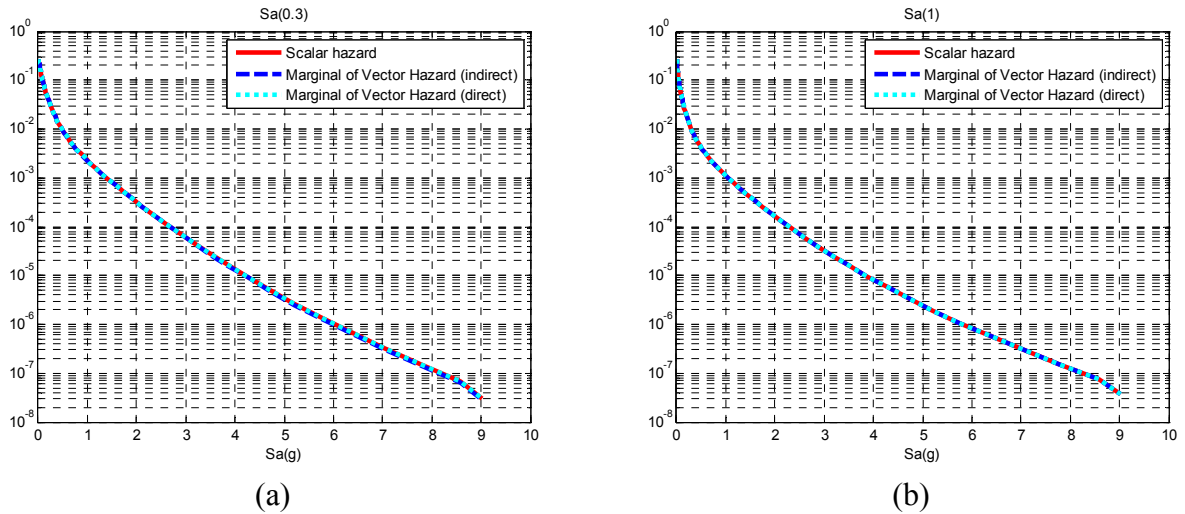**Figure 5** Ratio of the MAR in Figure 4b to the MAR in Figure 4a.

(a) (b)

Figure 6 Seismic hazard curves for (a) S_a(0.3s) and (b) S_a(1.0s) obtained via (1) a conventional scalar PSHA code, (2) the indirect approach and (3) the direct approach.

The insignificant discrepancies introduced by the indirect method in the conventional scalar seismic hazard curves (which are obtained from the 1D MAR) and in the joint 2D MAR are, of course, also found in the conditional hazard curves. This is apparent in Figure 7, which, as an example, shows the comparison of two conditional hazard curves for $S_a(0.3s)$, each of which is conditional to a different value of $S_a(1.0s)$. Incidentally, it is interesting to note the effect that the value of the conditioning variable has on the conditional hazard curves vis-a-vis the customary unconditional one (Figure 6a).
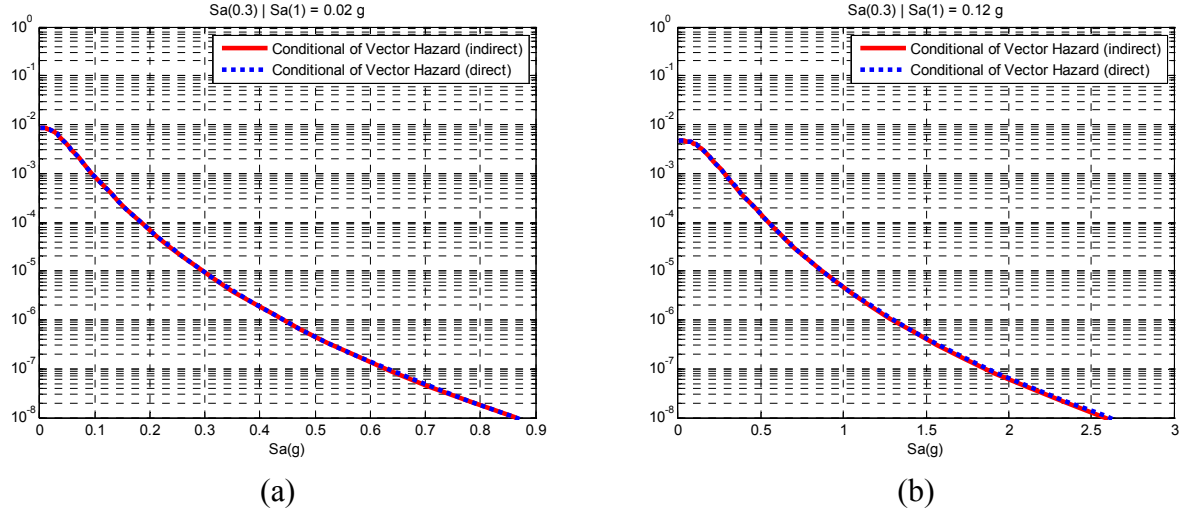

Figure 7 Comparison of two conditional hazard curves - (a) Conditional hazard of $S_a(0.3s)$ given $S_a(1.0s)$ equal to 0.02 g - (b) Conditional hazard of $S_a(0.3s)$ given $S_a(1.0s)$ equal to 0.12 g.

4.1.2 3D joint MAR of occurrence of $S_a(0.3s)$, $S_a(0.6s)$, and $S_a(1.0s)$

This section analyzes the accuracy of the indirect method for the joint 3D MAR of $S_a(0.3s)$, $S_a(0.6s)$, and $S_a(1.0s)$. Although not shown, the seismic hazard curve for the conditioning variable, $S_a(1.0s)$, is indistinguishable from that obtained via scalar PSHA (as was noted before for the 2D joint MAR) whereas the hazard curves for the two conditioned variables, $S_a(0.3s)$ and $S_a(0.6s)$, are within 3% of the exact values for the entire range of practical interest. Obviously, the 3D joint MAR cannot be displayed on paper; however, Figure 8 shows the contours of the joint 3D MAR obtained via the direct integration method for four different values. The joint 3D MAR from the indirect method, not shown here, is essentially identical. The contour values shown in Figure 8 are the 3D equivalent of the 2D contours displayed as rings of different colors in Figure 4.

As an example, one of the three 2D marginal MAR of the 3D MAR, obtained via both direct approach and indirect approach, is shown in Figure 9a and Figure 9b, respectively. Incidentally, note that the 2D marginal from the 3D direct integration is identical to the 2D joint that was shown in Figure 4a, which was obtained from the 2D direct approach. Figure 10 displays the ratio of the 2D $S_a(0.3s)$ and $S_a(1.0s)$ marginal MARs from Figure 9, which, as before, shows that the error is small where the MAR has noteworthy rate content and tends to be large for pairs of values that are extremely unlikely to occur jointly. A similar pattern and amplitude of errors was observed for the other two 2D marginal MARs, and therefore are not shown.

As for the 2D case, the analysis considers the approximation introduced by the indirect approach in several 2D conditional MARs. The consistency of the marginal MARs is, in fact, a necessary but not a sufficient condition for the consistency of the 3D joint MAR. Figure 11 shows the comparison of two 2D MARs of $S_a(0.3s)$ and $S_a(0.6s)$ extracted from the 3D joint MAR conditioned on $S_a(1.0s)$=0.02g (left

panels) and $S_a(1.0s)=0.12g$ (right panels). The error terms for both cases (panels e and f) mirrors the same kind of behavior of the errors in the 2D marginal MARs, namely that the error is very minor for practical situations and somewhat significant for combinations of values that are so unlikely to occur as to have no practical concern.

Given that both marginal and conditional 2D MARs have insignificant errors for all cases of practical interest, it is concluded that the joint 3D MAR from the indirect approach is also accurate. This was also confirmed by results of additional analyses, not shown here, on the ratio of the 3D joint MARs from direct and indirect approaches.
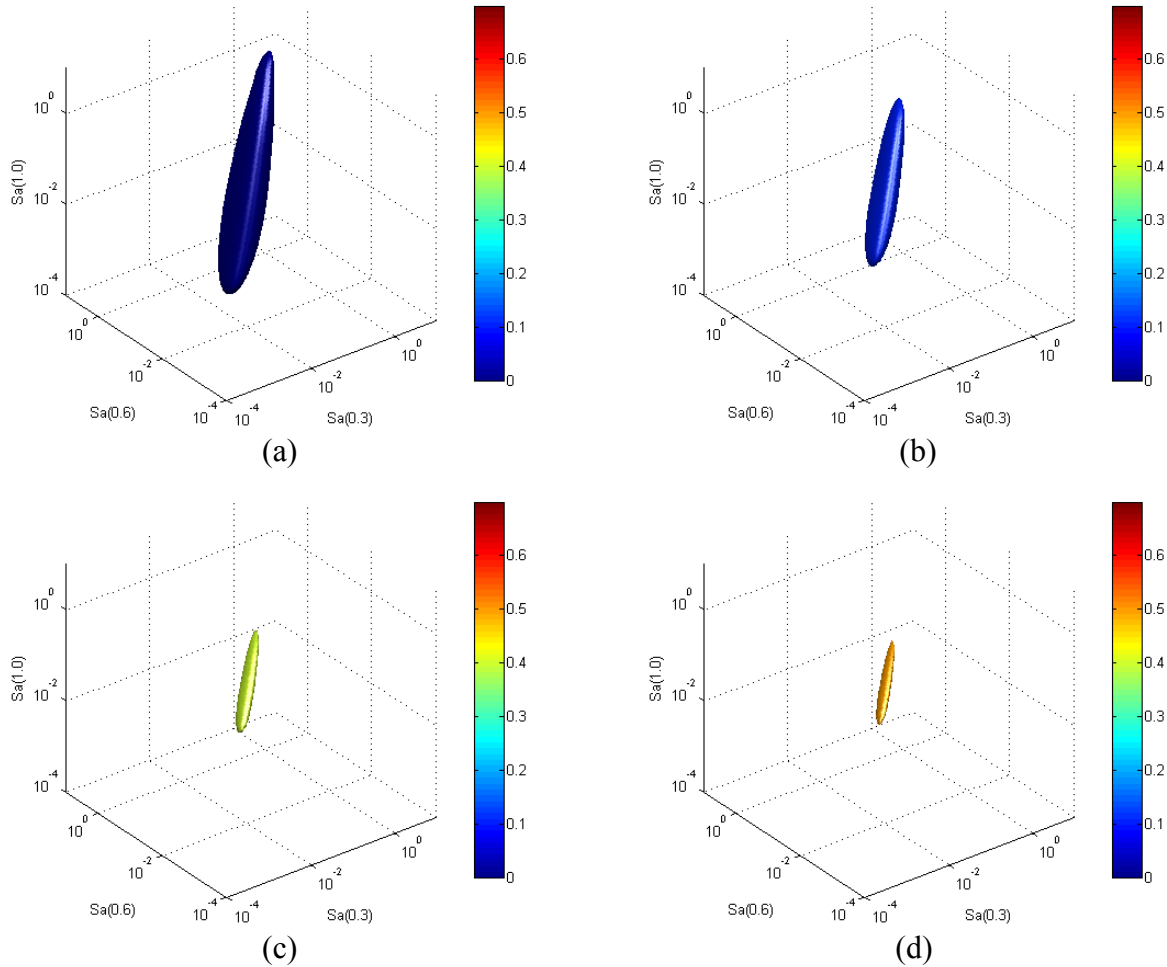

(a)

(b)

(c)

(d)

Figure 8 Contours of the 3D joint MAR of equaling triplets of $S_a(0.3s)$, $S_a(0.6s)$, and $S_a(1.0s)$ for four increasing MAR values: (a) 0.01×10^{-4}; (b) 0.1×10^{-4}; (c) 0.4×10^{-4}; and (d) 0.5×10^{-4}.

(a)   (b)
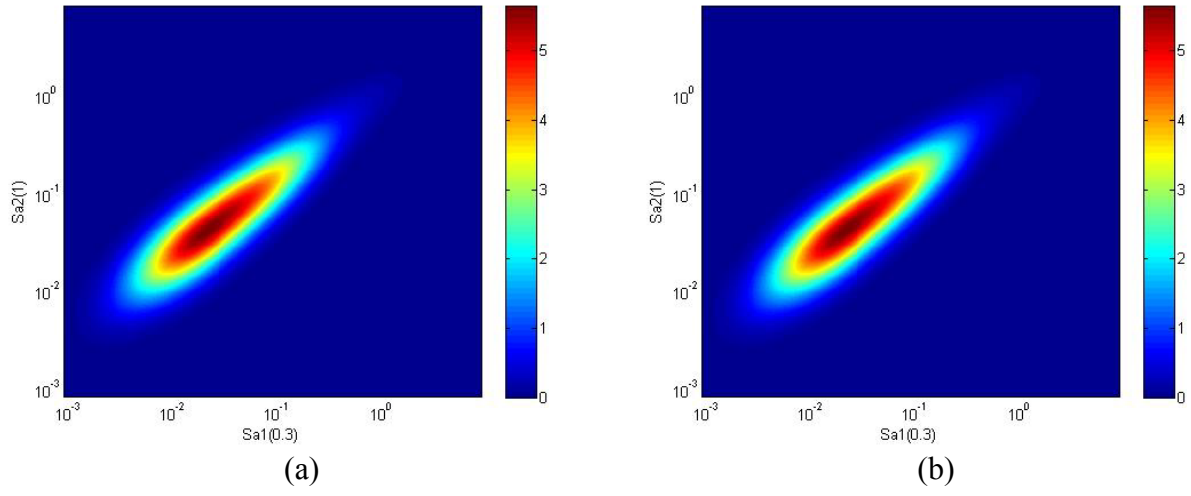
Figure 9 2D marginal MAR for S_a(0.3s) and S_a(1.0s) extracted from the 3D MAR computed via (a) the direct integration method and (b) the indirect method.
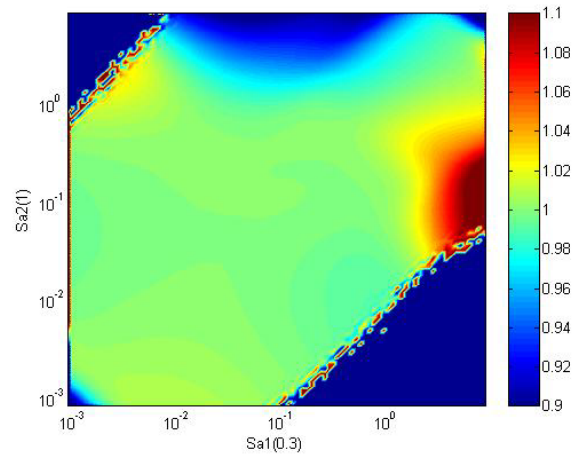

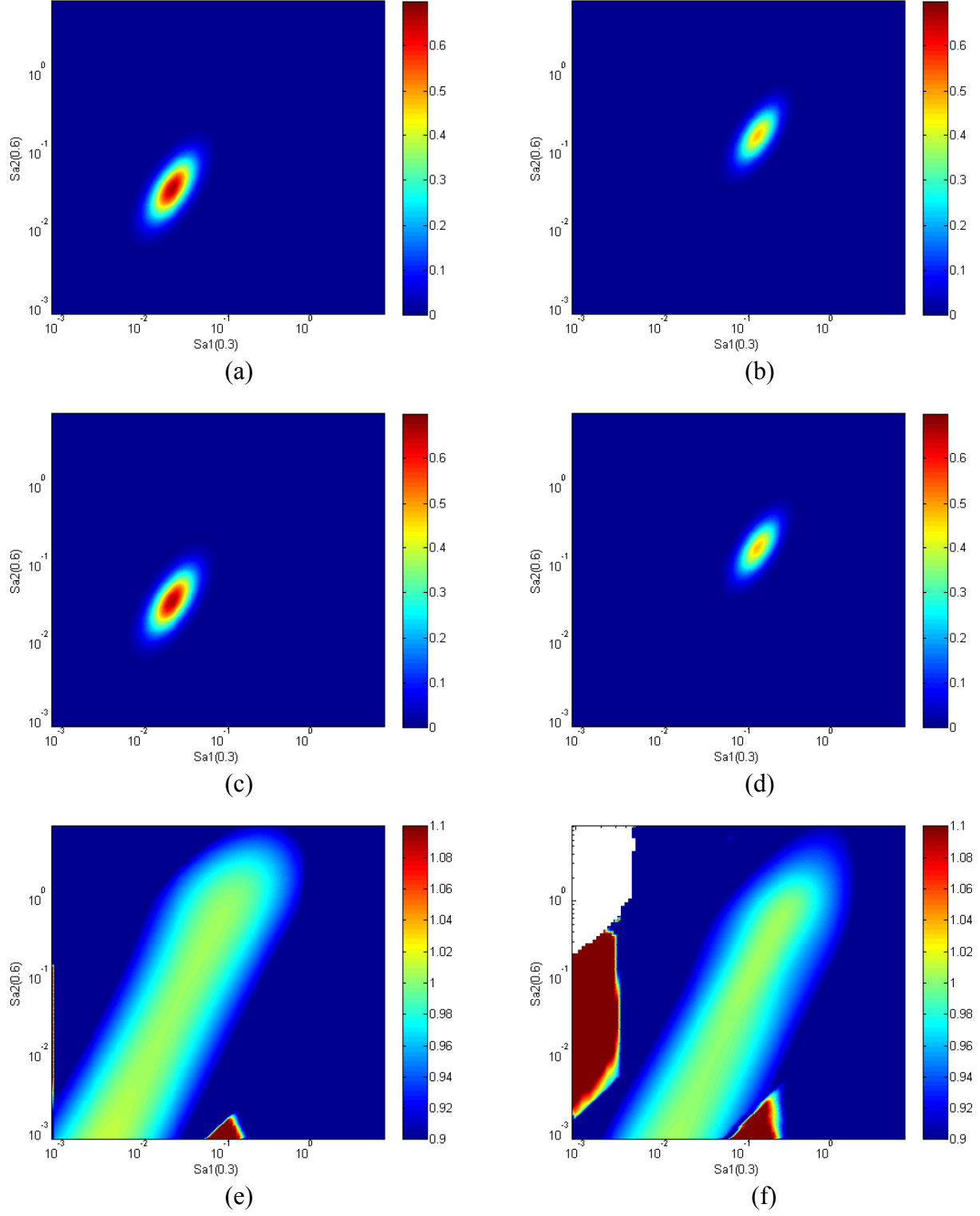**Figure 10** Ratio of the MAR in Figure 9b to the MAR in Figure 9a.

Figure 11 2D MARs of S_a(0.3s) and S_a(0.6s) extracted from the 3D joint MAR conditioned on S_a(1.0s)=0.02g (left panels) and S_a(1.0s)=0.12g (right panels). Panels (a) and (b) show the MAR computed via direct integration, panels (c) and (d) show the MAR computed via the indirect approach, and panels (e) and (f) show the ratio of the MARs.

4.1.3 4D joint MAR of occurrence of $S_a(0.3s)$, $S_a(0.6s)$, $S_a(0.9s)$, and $S_a(1.0s)$

This section analyzes the accuracy of the indirect method for the joint 4D MAR of $S_a(0.3s)$, $S_a(0.6s)$, $S_a(0.9s)$, and $S_a(1.0s)$. Although not shown, the seismic hazard curve for the conditioning variable, $S_a(1.0s)$, is indistinguishable from that obtained via a traditional scalar PSHA (as was also noted for the 2D and 3D Joint MAR), whereas the hazard curves for the three conditioned variables, $S_a(0.3s)$, $S_a(0.6s)$ and $S_a(0.9s)$, are within 3% of the exact values for the entire range of practical interest (e.g., see Figure 12). Obviously, the 4D joint MAR cannot be displayed on paper; however, Figure 13 shows the contours of the 3D marginal of 4D joint MAR obtained via the indirect approach, which is comparable to Figure 8. Figure 14a shows the 2D marginal MAR of the 4D MAR computed with the indirect approach, while Figure 14b shows the ratio of the 2D marginal MAR from the 4D MAR to the 2D joint MAR computed using the direct method as shown in Figure 9a. As indicated in Figure 14b, the error is small where the MAR has rate content of practical significance, and tends to be somewhat large for extremely unlikely pairs of values. It is practically impossible to compute a 4D joint MAR using the direct integration approach, but it can be concluded that the joint 4D MAR from the direct approach is accurate, as indicated by the results of additional analyses of the 3D marginal MAR of different variable pairs, as well as from 2D and scalar marginal comparisons.

Given that both marginal and conditional 2D MARs have insignificant errors for all cases of practical interest, it is concluded that the joint 4D MAR from the indirect approach is also accurate.
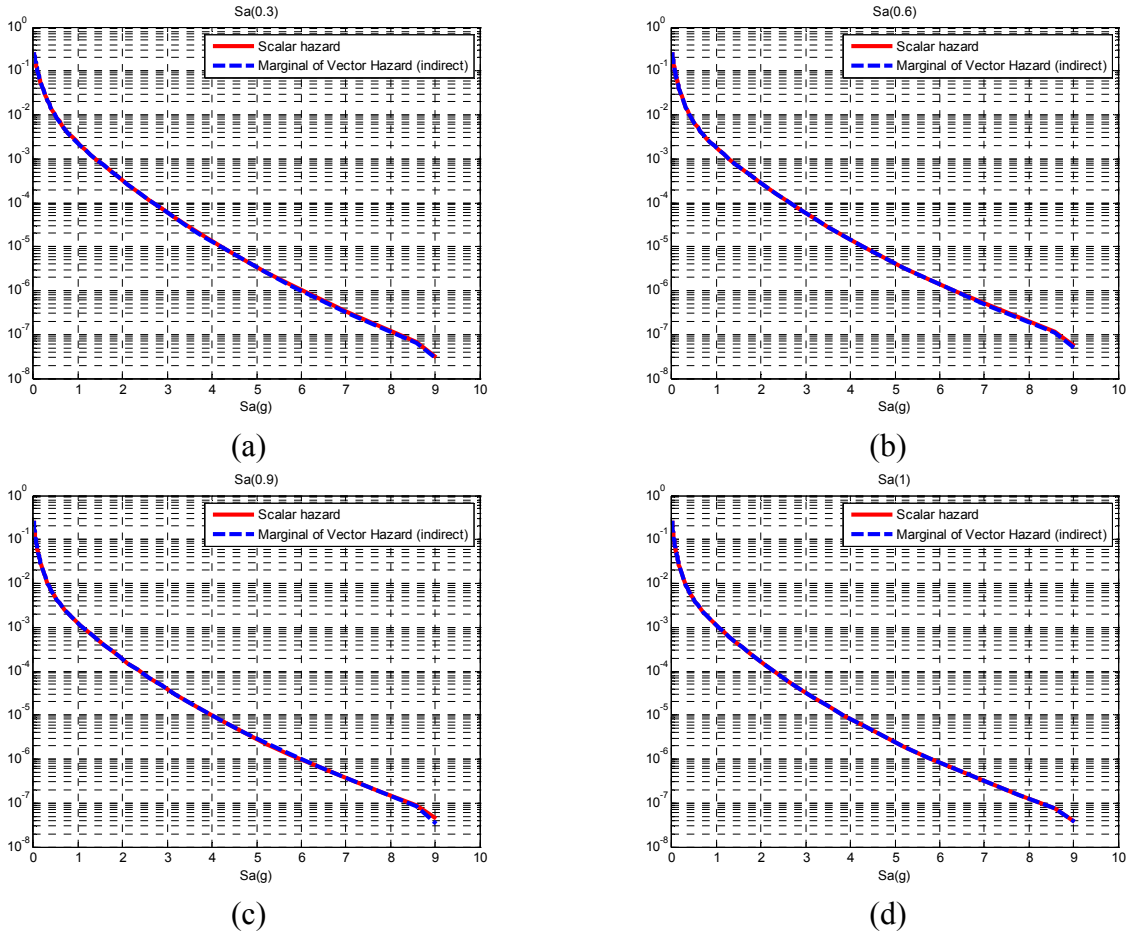

Figure 12 Seismic hazard curves for (a) $S_a(0.3s)$, (b) $S_a(0.6 s)$, (c) $S_a(0.9 s)$, and (d) $S_a(1.0s)$ obtained via a conventional scalar PSHA code and the indirect approach.

16

Figure 13 Contours of the 3D marginal of 4D joint MAR of equaling triplets of $S_a(0.3s)$, $S_a(0.6s)$, and $S_a(1.0s)$ for four increasing MAR values: (a) 0.01×10^{-4}; (b) 0.1×10^{-4}; (c) 0.4×10^{-4}; and (d) 0.5×10^{-4}.
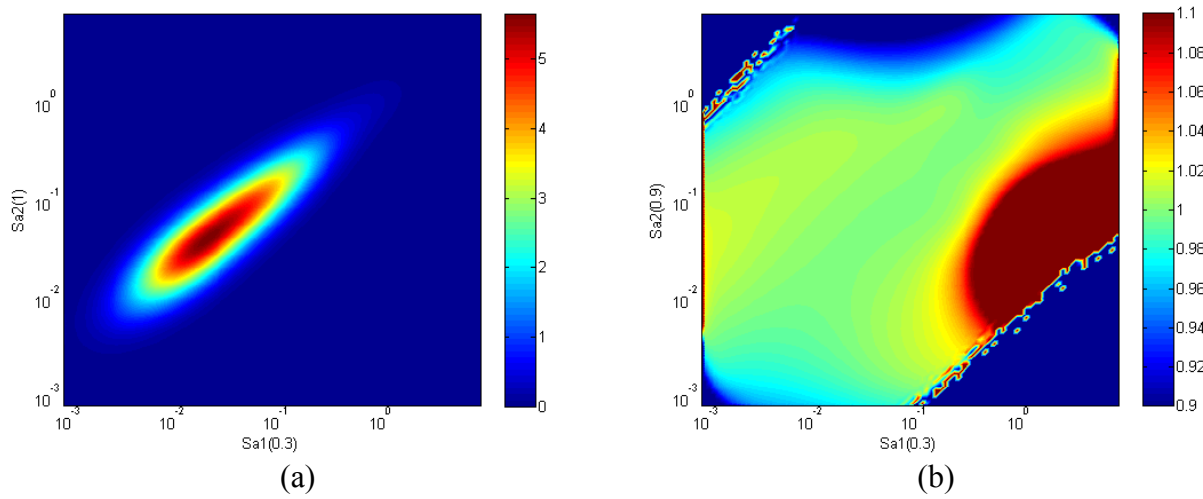

Figure 14 (a) 2D marginal MAR for $S_a(0.3s)$ and $S_a(1.0s)$ extracted from the 4D MAR computed via the indirect method. (b) Ratio of the MAR in Figure 14a to the MAR in Figure 9a.

17

4.1.4 5D joint MAR of occurrence of $S_a(0.3s)$, $S_a(0.6s)$, $S_a(0.9s)$, $S_a(1.0s)$, and $S_a(2.0s)$

This section analyzes the accuracy of the indirect method for the joint 5D MAR of $S_a(0.3s)$, $S_a(0.6s)$, $S_a(0.9s)$, $S_a(1.0s)$ and, $S_a(2.0s)$. This is the highest number of RVs for which VPSHA has ever been applied. As before for the 2D, 3D and 4D cases, the seismic hazard curve for the *conditioned* variable, $S_a(0.3s)$, is within 3% (for the entire range of practical interest) from that obtained via the "exact" scalar PSHA (Figure 15a). Furthermore, as shown in Figure 15b, the seismic hazard curve for the *conditioning* variable, $S_a(2.0s)$, is indistinguishable from that obtained via the scalar PSHA, whereas the hazard curves for the other three conditioned variables (not shown for brevity), $S_a(0.6s)$, $S_a(0.9s)$, and $S_a(1.0s)$ are also within 3% of the exact values for the entire range of practical interest. Given that the 1D marginals are in agreement with those obtained using the direct approach, we conclude that the marginals of higher dimensions and the 5D joint are also accurate.
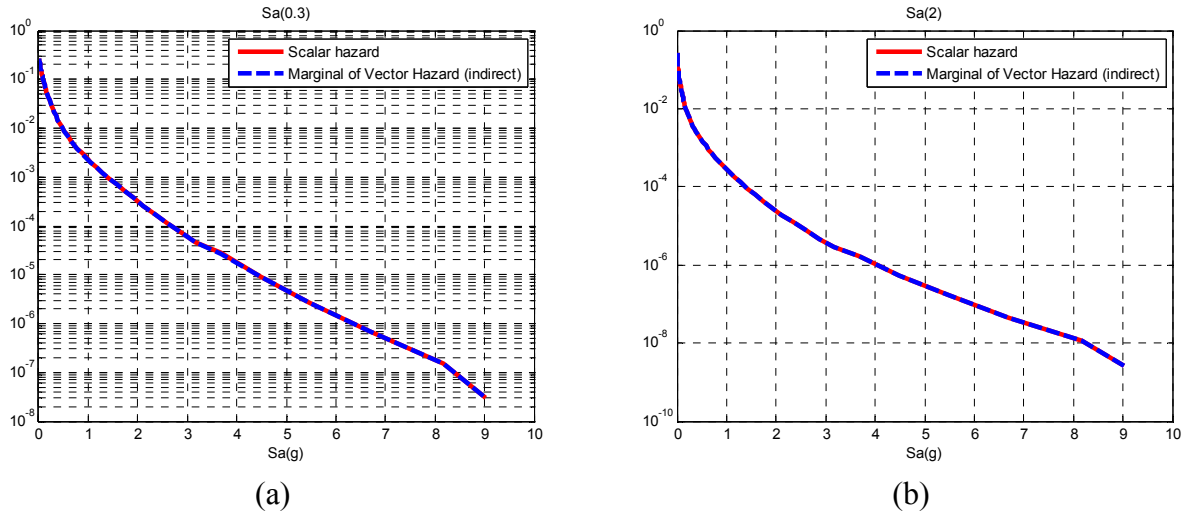

(a)   (b)

Figure 15 Seismic hazard curves for (a) the conditioned variable $S_a(0.3s)$ and (b) the conditioning variable $S_a(2.0s)$ obtained via (1) a conventional scalar PSHA code and (2) the indirect approach.

4.2 Van Nuys Holiday Inn site

The Van Nuys Holiday Inn site case study considers the same spectral quantities included in the Stanford University site case study but uses the state-of-the-art NGA equations by Boore and Atkinson (2008) to predict their values for shallow crustal earthquake ruptures of different mechanisms. The hazard disaggregation in the indirect method is performed for $X=[M, R,$ rupture mechanism] where R is the Joyner-Boore distance measure.

4.2.1 2D joint MAR of occurrence of $S_a(0.3s)$ and $S_a(1.0s)$

As shown by Figure 16, it is important to keep track of the rupture mechanism during hazard disaggregation for the indirect method, especially in complicated seismotectonic environments with many faults of different rupture mechanisms such as in Southern California. The $S_a(0.3s)$ seismic hazard curve shown as a dashed blue line in Figure 16a was obtained as the marginal of the 2D $S_a(1.0s)$ and $S_a(0.3s)$ MARs using the indirect method by assuming all ruptures are strike-slip mechanisms in the disaggregation procedure. The red and the cyan curves in Figure 16a, which are identical, were obtained using a scalar PSHA code and as a marginal of the 2D MAR obtained via the direct method. The error in estimating the rates of exceeding $S_a(0.3s)$ values of about 3.0g, which has a rate of exceedance lower than 10^{-4} at this site, is about 20% (Figure 16b). Unacceptable errors of similar magnitude can also be observed in the joint 2D MAR (not shown). It should be noted, however, that the error generated by

18

disaggregating the hazard with just M and R affects only the hazard curve of the conditioned variable(s) (e.g., $S_a(0.3s)$ in this case), but not those of the conditioning variable(s) (e.g., $S_a(1.0s)$ in this case). The results of the PSHA for the scalar conditioning quantity around which the entire indirect method pivots (see Eq. 3 and 4), is computed using the correct rupture mechanism for each event. This issue will be addressed in more detail in Section 5.
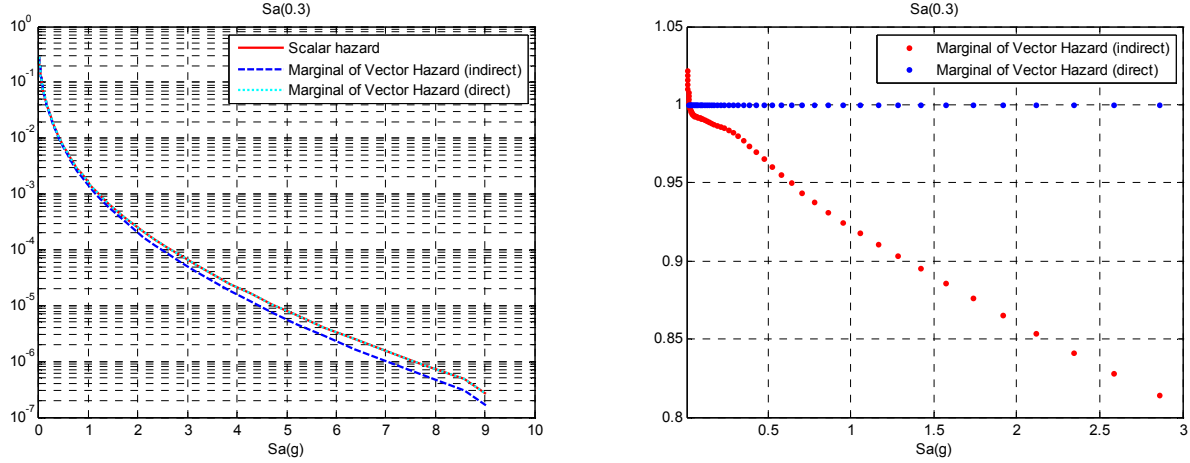

Figure 16 Effects of disregarding the rupture mechanism on the accuracy of the hazard curve obtained for the conditioned variable $S_a(0.3s)$ using the indirect method (blue dashed line in Panel a). Panel b shows the ratio of the hazard curves obtained via direct method (blue dots) and indirect method (red dots) to the hazard curve computed via scalar PSHA.

When the rupture mechanism is correctly included in the disaggregation, the approximation in the hazard results provided by the indirect method improves dramatically, as shown in Figure 17a for the 1D case and Figure17b for the 2D case. For example, the approximation is below 5% at the 3g $S_a(0.3s)$ level for the scalar case. All the remaining analyses carried out herein for the Van Nuys site will include the rupture mechanism in the hazard disaggregation.

(a)   (b)

Figure 17 Accounting for the rupture mechanism during hazard disaggregation improves significantly the accuracy of the hazard curve computed via the indirect method. Panel a shows the ratio of the hazard curves for $S_a(0.3s)$ obtained via direct method (blue dots) and via indirect method (red dots) to the hazard curve computed via scalar PSHA. Panel b displays the Ratio of the 2D MAR computed via the indirect method to the 2D MAR computed via direct ("exact") method.

19

The accuracy of the joint 3D hazard computed using the indirect method is comparable with what was presented previously for the 2D case and for the Stanford University site. The error introduced in the scalar hazard of the conditioned variables is no larger than a few percent at large spectral values corresponding to mean return periods of 10,000 years or longer. The 2D marginal and conditional MARs produced by the indirect method show, again, that the error is within 3% for all pairs of values with non-negligible joint rates of occurrence. As an example, Figure 18 shows the ratios of 1D and 2D hazard results obtained via the indirect and direct methods.
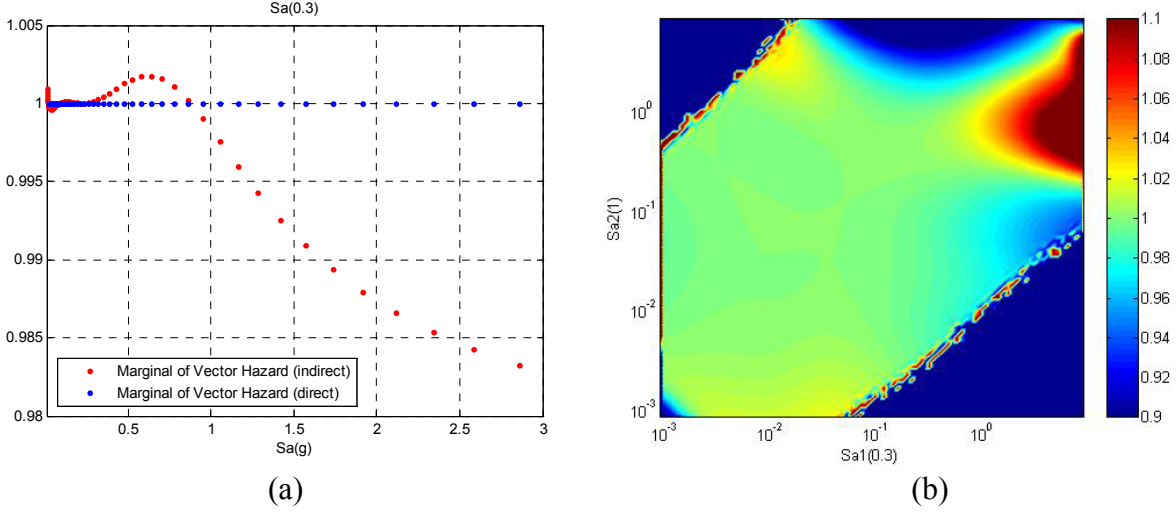

(a)   (b)

Figure 18 Approximation introduced by the indirect method for VPSHA calculations - (a) the ratio of the hazard curves for S_a(0.3s) obtained via direct method (blue dots) and via indirect method (red dots) to the hazard curve computed via scalar PSHA (b) the ratio of one of the 2D marginal of 3D Joint MAR to 2D MAR via direct method.

5. Sensitivity of Domain Discretization to Input RVs of Joint Hazard Results obtained via the Indirect Method

The results from the indirect method up to three RVs presented in Section 4 were obtained, by design, using a large number of bins to discretize the domain of each random variable. The large number of bins, however, made these analyses for a number of RVs larger than three so computationally costly as to be incompatible with budget and timeline of most real applications. Also, for 4D and higher dimension cases the data storage requirements generated by this large number of bins becomes excessive. Therefore, using a less refined discretization becomes a necessity for certain applications.

The accuracy of the indirect method, however, may suffer from coarse discretization of the domain of the random variables considered (i.e., *M*, *R*, and other IMs). During the computations, the GMPE evaluation is performed using the mean value of each bin. This method groups many different ruptures with *similar values* of the variables *X* into one single bin and, if the bin sizes are too wide, the mean value *x* of the bin *X* may not accurately represent some of the events in the bin and could potentially yield inadequate ground motion estimates. Similarly, the calculation of the conditional distributions of the various IMs in Eqs. 3 and 4 is carried out on the mean value of the bin of the conditioning IMs (e.g., S_{a2} and S_{a3} in Eq. 3). Again, if the number of IM bins is too small, the accuracy of the joint hazard may be impacted beyond acceptable thresholds.

This section investigates the errors introduced by using a smaller number of bins for each random variable (both *X* and the IMs) to the joint hazard estimates obtained via the indirect method. The Stanford

20

University site joint hazard results from one to three IMs (see Subsection 4.1) obtained using the direct integration method are used as a benchmark for the indirect method results computed using different cases with varying number of bins.

5.1 Sensitivity of the 2D $S_a(0.3s)$ and $S_a(1.0s)$ MAR

The sensitivity analysis on the bin number considers eight cases with uniform bins (denoted as A through H in Table 1) and 13 cases with variable-size bins (denoted as 1 through 13 in Table 1) judiciously selected on the basis of the hazard disaggregation results for the site and on the range of IMs of practical interest. Table 1 shows the details of the number of bins for each variable and the computation time (in minutes), while Figure 19 and Figure 20 show the error of the results introduced by the coarser discretization of the domain. In the realm of the uniform bin discretization, Case H is superior to the other cases as it provides acceptable results and a very short computation time. The errors are negligible for most of the IMs' range of practical interest, and approach 10% at approximately 3g, which is a value with less than 10^{-4} mean annual rate of exceedance for this site (see Figure 19). Although cases A-H are appealing because of their simplicity, superior results with equal or less computational effort can be obtained by a careful selection of non-uniform bin sizes for M, R, and the IMs. Figure 20 shows the error in the MAR of the conditioned variable, here $S_a(0.3s)$, compared to the benchmark results. The errors in the MAR of the conditioning variable are not shown because they are smaller. Cases 9, 10, 12, and 13 have errors below 3% at 3g and a competitive computation time, and thus are superior to the all the other cases. These cases will also be used for higher dimensions in the following subsections.

Table 1 Details of the 2D sensitivity cases considered to test the accuracy of the hazard estimates for different choices of M, R, and IM bin selections.

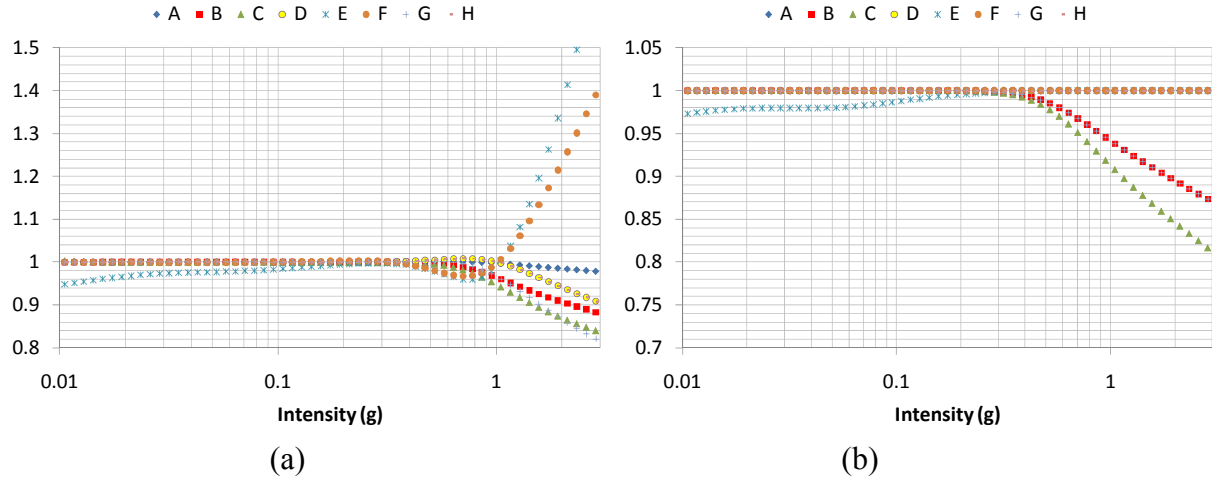| Case		Number of Bins			Computation Time (minutes)
		Magnitude	Distance	Intensity	
Uniform Bin Size	Base	160	101	93	2.58
	A	64	101	93	0.97
	B	32	101	93	0.50
	C	16	101	93	0.25
	D	160	41	93	0.97
	E	160	29	93	0.68
	F	160	21	93	0.50
	G	32	41	93	0.20
	H	64	41	93	0.40
Selective Bin Size	1	82	101	93	1.33
	2	70	101	93	1.13
	3	62	101	93	1.00
	4	32	101	93	0.52
	5	22	101	93	0.35
	6	161	61	93	1.62
	7	161	56	93	1.52
	8	161	26	93	0.68
	9	70	61	93	0.68
	10	32	61	93	0.32
	11	161	101	68	1.42
	12	32	61	68	0.17
	13	70	61	68	0.37

Figure 19 Error in MAR of (a) the conditioned variable, $S_a(0.3s)$ and (b) the conditioning variable, $S_a(1.0s)$ computed as the marginal of the bi-variate vector hazard analysis for cases A-H. The curves represent the ratio of the marginals obtained from the bi-variate analysis to the scalar results.
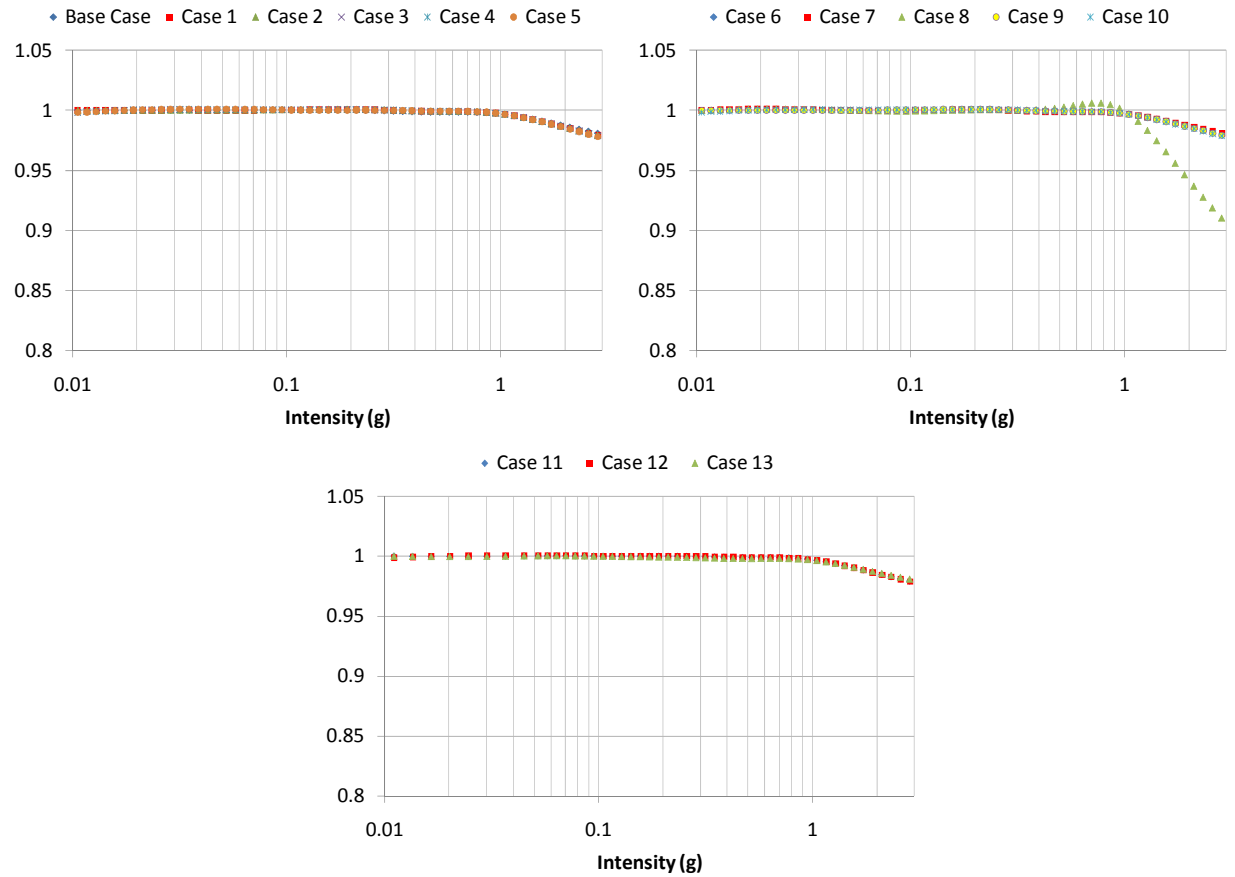

Figure 20 Error in MAR of the conditioned variable, $S_a(0.3s)$, computed as the marginal of the bi-variate vector hazard analysis for cases 1-13. The curves represent the ratio of the marginals obtained from the bi-variate analysis to the scalar results.

5.2 Sensitivity of the 3D S_a(0.3s), S_a(0.6s), and S_a(1.0s) MAR

The sensitivity analysis for the tri-variate case of the MARs of the conditioned variables S_a(0.3s) and S_a(1.0s) presented in Table 2 is shown in Figure 21. The careful selection of the bins limits the error to less than 3% in the entire range between 0 and 3g. The error in the conditioning variable S_a(0.6s), which is not shown, is even smaller.

Table 2 Details of the 3D sensitivity cases considered to test the accuracy of the hazard estimates to different choices of *M, R*, and IM bin selections. The case numbers are consistent with the 2D cases listed in Table 1.

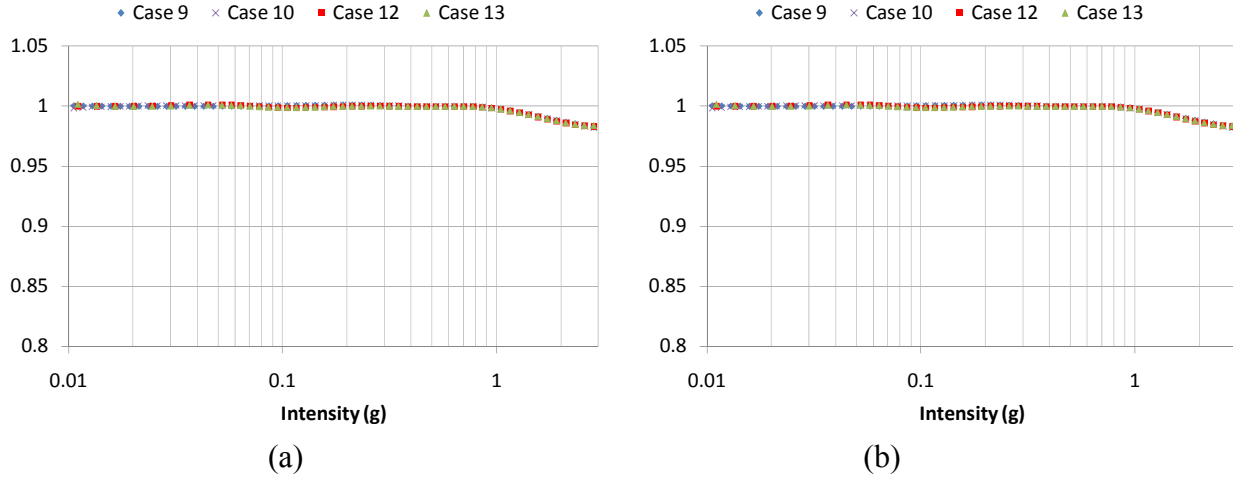| Case	Number of Bins			Computation Time (minutes)
	Magnitude	**Distance**	**Intensity**	
9	70	61	93	53.78
10	32	61	93	24.58
12	32	61	68	9.33
13	70	61	68	21.37

Figure 21 Error in the MAR of the conditioned variables, (a) S_a(0.3s) and (b) S_a(1.0s), computed as the marginal of the tri-variate vector hazard analysis for cases 9, 10,12 and 13. The curves represent the ratio of the marginals obtained from the tri-variate analysis to the scalar results.

5.3 Computer Run Times of the Higher Dimension Cases

Results of the 3D sensitivity analysis were used to inform the choice of the bin size selected in the 4D and 5D indirect method cases run for the Stanford University site case study discussed in Subsections 4.1.3 and 4.1.4. An appropriate bin configuration and size was applied in an attempt to minimize the computer run time without compromising the accuracy of the joint hazard estimates. For example, the run time of the 4D case was about 900 hours, using the selective bin size case "13" outlined in Table 1. The run time of the 5D case was about 3,000 hours, using the selective bin size case "12" outlined in Table 1. Note that these run times refer to modern desktop computers with at least 2GHz processing speed. In reality, we carried out the actual computation using multi-processors computers.

6. Disaggregation of Multi-Variate Joint Hazard

A general improvement of the VPSHA methodology is the ability to compute the contributions to the joint hazard in terms of the M, R, and, if needed, the rupture mechanism of the causative events. Although not implemented here, the joint hazard disaggregation can be easily extended to identify the latitude and longitude of the events, so that the specific faults that control the hazard can be uniquely recognized (Bazzurro and Cornell, 1999). Several refinements of the disaggregation exercise can be carried out to meet the requirements of the users. For example, in a 2D joint hazard case, the disaggregation can be implemented to extract the contributions to the MAR of "equaling" a certain joint IM cell (e.g., $S_a(0.3s)=0.2g$ and $S_a(1.0s)=0.1g$), or to the MAR of equaling or exceeding it (e.g., $S_a(0.3s) \geq 0.2g$ and $S_a(1.0s) \geq 0.1g$). These two cases are shown in Figure 22. Other variations of this 2D disaggregation scheme are also possible, such as disaggregation of the 1D MAR of an IM (e.g., $S_a(0.3s) = 0.8g$) conditional on the second IM exceeding a certain value (e.g., $S_a(1.0s) \geq 0.5g$).
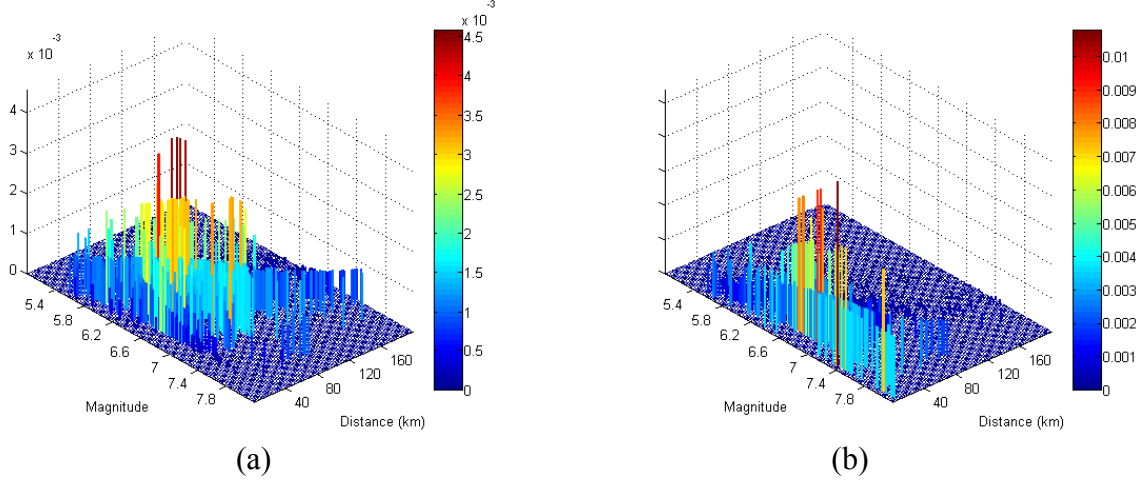

(a)   (b)

Figure 22 Disaggregation of the 2D MAR of (a) $S_a(0.3s)=0.2g$ and $S_a(1.0s)=0.1g$ and (b) of $S_a(0.3s) \geq 0.2g$ and $S_a(1.0s) \geq 0.1g$ at the Stanford University site discussed in Subsection 4.1.

If required, the disaggregation of the joint hazard can be easily performed for a higher number of dimensions. For instance, the 3D MAR of equaling or exceeding the values identifying a specific cell, or the conditional 2D MARs of the tri-variate joint, can also be disaggregated. As an example, Figure 23 shows the disaggregation of the marginal 2D $S_a(0.3s)$ and $S_a(0.6s)$ MAR of the 3D case conditional on $S_a(1.0s)$, equaling or exceeding 0.2 g.
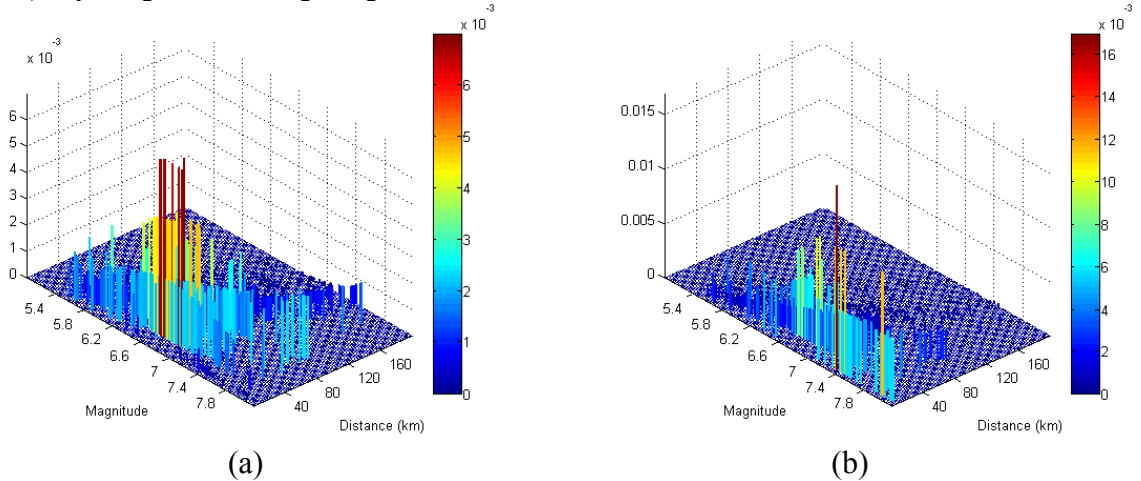

(a)   (b)

Figure 23 Disaggregation of the 2D $S_a(0.3s)$ and $S_a(0.6s)$ MAR conditional on the third IM, $S_a(1.0s)$, (a) equaling 0.2 g and (b) exceeding 0.2 g.

24

7. Summary and Conclusions

This study presents two parallel methods of Vector-valued PSHA (VPSHA) that allow the computation of the joint seismic hazard for a number of IMs larger than ever before. The two methods presented are (1) the conceptually straightforward, but numerically challenging, *direct integration method* and (2) the mathematically complex, but more computationally efficient, *indirect method*. With modern desktop computing environments, the former method can accommodate up to three IMs while the latter method can accommodate up to 5 or 6 IMs with joint hazard estimates that are within a very acceptable level of accuracy for most practical applications. To the authors' knowledge, the few available VPSHA computer codes could, until now, only compute the joint hazard of two IMs.

The main focus of this study was to investigate the use of the indirect method, which is a novel and versatile approach to VPSHA that utilizes the standard results from standard scalar PSHA analyses and information about the correlation of the ground motion IMs for which the joint mean rate density, MRD (or equivalently, the joint mean annual rate, MAR) is sought. More clearly, the indirect method needs (a) the variance-covariance matrix of the IMs of interest, which is available in the literature for the most common IMs such as PGA and spectral quantities, (b) the standard PSHA hazard curves and (c) hazard disaggregation results from a series of scalar PSHAs obtained for the same IMs via the use of any standard PSHA code of choice. The implementation of the indirect method to VPSHA removes the main obstacles that have so far prevented an easy computation of joint hazard by earth scientists and a straightforward use by engineers of multiple response measures in response assessment of 2D and 3D representations of structures.

While both methods have their respective strengths and weaknesses, the indirect method has several qualities that, arguably, make it superior to the direct integration method. The benefits of the indirect method are listed as follows:

- Its implementation does not require much modification of existing scalar PSHA codes.
- It can accommodate a higher number of IMs than the direct method.
- It is computationally faster than the direct method for two reasons:
  - Integrating multi-variate standard normal distributions with three or more dimensions with very high accuracy is typically an extremely time consuming task. The indirect method has other mathematical challenges, such as matrix inversions, which, however, require considerably lower computation time[2].
  - Multi-dimension integration needs to be repeated for every earthquake considered in the PSHA. In the indirect method, the number of events affects only the total run time of the scalar hazard analyses, which is negligible when compared to the the total run time of a joint hazard study.
- It is easily scalable to higher dimensions of variables. Given its recursive nature, when adding the *n*-th dimension, the indirect method can re-use results previously computed for the first *n*-1 dimensions. Conversely, adding an additional dimension in the direct method requires restarting the hazard analysis.

The weaknesses of the indirect method include:

- It requires larger computer memory space than the direct method.
- It yields results that are approximate when the number of bins used to discretize the domains of the RVs is limited, which is necessary in applications with four or more IMs. However, an extensive sensitivity analysis carried out in this study has shown that a judicious selection of bins

---

[2] Matrix inversion is performed herein using the Cholesky factorization and back substitution algorithm (Trefethen and Bau, 1997)

guided by disaggregation results can limit the error in the estimates of the joint and marginal MARs computed by the indirect method to values typically lower than 3% for the entire IMs of engineering significance.

The direct integration method appears to be superior to the indirect method only when one seeks to compute the joint MAR within a confined region of the joint domain of all the IMs considered (e.g., S_a(0.3s), S_a(0.6s) and S_a(1.0s) between 0.5g and 1.0g). For any situation, the indirect method requires the computation of the joint hazard for the *entire* domain of the IMs. However, no practical applications are immediately apparent that would require such limited knowledge of the joint hazard.

This study has also presented the disaggregation of the joint hazard for M, R, and the rupture mechanism for 2D and 3D cases. The disaggregation is presented for both (a) the mean annual rate of equaling and (b) the mean annual rate of exceeding a joint set of IM values. These disaggregation results can be useful in many applications, such as ground motion record selection for engineering analyses. Note that the disaggregation plots shown herein are obtained using the indirect method; however, the same results may be obtained by disaggregating the joint hazard computed via the direct integration approach as well.

Finally, it is emphasized that the indirect method may be easily coupled with existing PSHA procedures, including the hazard and disaggregation results from USGS scalar hazard maps or from OpenSHA, to produce *joint* hazard estimates of different combinations of ground motion parameters at any site. It is possible to envision an interactive tool on the USGS website that would enable a user to input the coordinates (or ZIP code) of a building site, specify the periods of the first modes of vibration along the principal axes of the building (i.e., T_L and T_T), identify the direction of the building's principal axes with respect to geometric north, and obtain plots and tables with joint rates of exceedance for different pairs of values of $S_a(T_L)$ and $S_a(T_T)$. Some of the tables could, for example, list all the $S_a(T_L)$ and $S_a(T_T)$ pairs whose joint exceedance is equal to some common target value, such as 10% in 50 years. With additional information of the target exceedance rate (e.g., 10% in 50 years), and a pair of $S_a(T_L)$ and $S_a(T_T)$ values taken from one of the provided tables, the user could obtain a plot of the disaggregated magnitude and distance pairs of the scenarios that most contribute to the target exceedance rate at any site. Such a tool, which is based on the VPSHA method discussed herein, is potentially valuable for both design and performance evaluation of buildings and other structures. Similar applications in geotechnical engineering, such as slope stability or liquefaction assessment studies, may also benefit from customizable VPSHA results easily available from a USGS web-based application.

8. References

Abrahamson, N. and Silva W. (1997). "Equations for estimating horizontal response spectra and peak acceleration from West North American Earthquakes: A summary of recent work", *Seismological Research Letters*, 68, 94-127.

Abrahamson, N., Atkinson, G., Boore, D., Bozorgnia, Y., Campbell, K., Chious, B., Idriss, I.M., Silva, W., Youngs, R., (2008). "Comparisons of the NGA Ground-Motion Relations", Earthquake Spectra 24 (1), 45-66.

Baker, J.W. and Cornell, C.A. (2006). "Correlation of Response Spectral Values for Multi-Component Ground Motions", Submitted to *Bulletin of Seismological Society of America* (B.S.S.A.), 96 (1), 215-227.

Baker, J.W. and Jayaram N. (2008). "Correlation of spectral acceleration values from NGA ground motion models," Earthquake Spectra, 24 (1), 299-317.

Bazzurro, P. (1998). "Probabilistic Seismic Demand Analysis", Ph.D. Dissertation, Dept. of Civil and Environmental Engineering, Stanford University, Stanford, CA, August.

Bazzurro, P., and C.A. Cornell (1999). ``Disaggregation of Seismic Hazard". *Bulletin of Seismological Society of America (B.S.S.A.)*, Vol. 89, No. 2, April, pp. 501-520.

Bazzurro, P., and Cornell, C.A. (2001). "Vector-valued Probabilistic Seismic Hazard Analysis". *Seismological Research Letters*, Vol. 72, No.2, March/April, p. 273.

Bazzurro, P., and Cornell, C.A. (2002). "Vector-valued Probabilistic Seismic Hazard Analysis (VPSHA)". *Proceedings of 7th U.S. National Conference on Earthquake Engineering*, Boston, MA, July 21-25, Paper No. 61.

Bazzurro, P., and Luco, N. (2004). "Parameterization of Non-Stationary Acceleration Time Histories". Task 1", PEER Report, Task 1G00, Agreement No. SA 3592, University of California at Berkeley, Berkeley, CA.

Bazzurro, P. and Luco, N. (2005). "Beyond Spectral Quantities to Improve Structural Response Estimation", unpublished manuscript (copy available upon request).

Boore, D.M. and Atkinson, G.M. (2008). "Ground-motion prediction equations for the average horizontal component of PGA, PGV, and 5%-damped PSA at spectral periods between 0.01 s and 10.0 s", *Earthquake Spectra*, 24, 99 – 138, EERI.

Deierlein, G.G., Krawinkler, H. and Cornell, C.A. (2003) "A framework for performance-based earthquake engineering". *Pacific Conference on Earthquake Engineering*. University of Canterbury, Christchurch, New Zealand.

Genz, A. and Bretz F. (1999) "Numerical Computation of Multivariate t Probabilities with Application to Power Calculation of Multiple Contrasts", *J. Statist. Comput. Simul.*, 63:361-378.

Genz, A. and Bretz F. (2002) "Comparison of Methods for the Computation of Multivariate t Probabilities", *J. Comp. Graph. Stat.*, 11(4):950-971.

Goda K., Hong H.P. (2008). "Spatial correlation of peak ground motions and response spectra", *Bulletin of the Seismological Society of America,* 98(1): 354-365.

Gülerce, Z., and Abrahamson, N.A. (2010) "Vector-valued Probabilistic Seismic Hazard Assessment for the Effects of Vertical Ground Motions on the Seismic Response of Highway Bridges", *Earthquake Spectra* EERI. (Accepted in publication)

Inoue, T. (1990). "Seismic Hazard Analysis of Multi-Degree-of-Freedom Structures", *Rept. RMS-8*, Dept. of Civil and Environmental Engineering, Stanford University, Stanford, CA. July.

Jayaram N. and Baker J.W. (2008). "Statistical tests of the joint distribution of spectral acceleration values," Bulletin of the Seismological Society of America, 98 (5), 2231-2243.

Luco, N., and Cornell, C.A. (2000). "Effects of Connection Fractures on SMRF Seismic Drift Demands", *ASCE Journal of Structural Engineering*, 126(1): 127-136), January.

Luco, L., Manuel, L., Baldava, S., and Bazzurro P. (2005a). "Correlation of Damage of Steel Moment-Resisting Frames to a Vector-valued Ground Motion Parameter Set that includes Energy Demands", *Report prepared for U.S. Geological Survey (USGS)*, Award No. 03HQGR0057, February.

Luco, L., Manuel, L., Baldava, S., and Bazzurro P. (2005b). "Correlation of Damage of Steel Moment-Resisting Frames to a Vector-Valued Set of Ground Motion Parameters", Accepted for publications in *Proceedings of the 9th ICOSSAR05*, June 19-22, Rome, Italy.

Luco, N., and Cornell, C.A. (2007). "Structure-Specific Scalar Intensity Measures for Near-Source and Ordinary Earthquake Ground Motions", *Earthquake Spectra*, Vol. 23, No. 2, pp. 357-392.

Maffei, J., and Yuen N. (2007). "Seismic Performance and Design Requirements for High-rise Concrete Buildings", *Structure Magazine*, April.

Thio, H.K. (2003). Personal communication, URS Corporation, Pasadena, CA, July.

Trefethen, L.N. and Bau D. III, "Numerical Linear Algebra", *SIAM*, 1997, ISBN, 0-89871-361-7.